



---

Ao. Prof. Dr. Gernot Tragler

## DIPLOMARBEIT

---

# Optimal Dynamic Management of the Population Mix: Application of the OCMat Toolbox

---

Ausgeführt am Institut für  
WIRTSCHAFTSMATHEMATIK  
der Technischen Universität Wien

unter der Anleitung von  
Ao. Prof. Dr. Gernot Tragler  
und  
Dr. techn. Dieter Grass  
als verantwortlich mitwirkenden Universitätsassistenten

durch  
Reka Horvath  
Liniengasse 18/19, 1060 Wien

Wien, am 15. September 2011

---

Verfasserin



## Erklärung

Hiermit versichere ich, dass ich die vorliegende Arbeit selbständig verfasst und keine anderen als die angegebenen Quellen und Hilfsmittel benutzt habe, dass alle Stellen der Arbeit, die wörtlich oder sinngemäß aus anderen Quellen übernommen wurden, als solche kenntlich gemacht sind, und dass die Arbeit in gleicher oder ähnlicher Form noch keiner Prüfungsbehörde vorgelegt wurde.

Wien, am 15. September 2011

---

Verfasserin

Reka Horvath  
Liniengasse 18/19  
1060 Wien  
reka.horvath@gmx.at

**Abstract** This thesis presents a mathematical approach and theoretical treatment of a central challenge of modern housing policy: deconcentrating poverty via “housing mobility programs”. The idea is to move poor families into middle-class neighborhoods without inducing the inhabitants of these communities to outward migration or “flight”. The emphasis is put on the search for an optimal compromise between preserving the established population in a neighborhood and facilitate the inflow of marginalized families. The problem is treated by methods of optimal control theory using the MATLAB® toolbox OCMat developed by Dieter Grass (currently project assistant in the research unit for Operation Research and Control Systems at the Vienna University of Technology). The analyzed scenarios exhibit unique solutions but also cases of indifference, for which two optimal solutions exists.

**Keywords** Dynamic segregation · Nonlinear optimal control · OCMat Toolbox · Indifference point

# Contents

<b>Contents</b>	<b>3</b>
<b>1 Introduction</b>	<b>5</b>
<b>2 Policy Context</b>	<b>7</b>
2.1 The USA in words and figures . . . . .	7
2.2 Fighting segregation in Europe . . . . .	11
<b>3 The Model</b>	<b>15</b>
<b>4 The MATLAB-Toolbox: OCMat</b>	<b>21</b>
<b>5 Analysis of the Dynamical System</b>	<b>23</b>
5.1 Introductory analysis . . . . .	23
5.2 Phase portrait . . . . .	28
5.3 Bifurcation diagrams . . . . .	33
5.4 Indifference points . . . . .	56
5.5 From base case to case of indifference . . . . .	61
<b>6 Summary and Policy Conclusions</b>	<b>67</b>
 <b>List of Figures</b>	 <b>70</b>
 <b>List of Tables</b>	 <b>72</b>
 <b>Bibliography</b>	 <b>73</b>



## Introduction

This thesis deals with the problem faced by a social planner who wants to integrate a stream of poor families into a middle-class area without evoking middle-class flight. Placing too many poor families in a short time would induce current residents to emigrate and even deter other affluent residents from moving in. Both possibilities would reduce the tax base of the community to which the poor families are relocated, and that is counterproductive. But placing too few marginalized families squanders the opportunity to use the resources of the community to help to assimilate poor families into middle class.

This problem has very concrete, practical motivations. It has received considerable attention in academic research including the analysis of group effects, social interactions and networks, in particular with respect to the design of efficient social policies. However, this kind of problem has rarely been addressed with powerful analytic methods such as optimal control applied in the present work.

Social interactions are mathematically closely associated with non-linearities and multiple equilibria. The existence of multiple equilibria is related to the existence of so-called Skiba or DNSS points. Multiplicity means that for given initial states there exist multiple optimal solutions; thus the decision-maker is indifferent about which option to choose, i.e., at such a threshold different optimal paths exist. Small movements away from the threshold typically resolve the indifference and lead to a unique optimal solution. Sethi (1977, 1979), Skiba (1978) and Deckert and Nishimura (1983) explored these points of indifference for the first time when they considered a special class of optimal control problems. In recognition of their studies these points of indifference are denoted as DNSS (Deckert-Nishimura-Sethi-Skiba) or simply Skiba points.

The following work analyzes the strategy of a housing mobility program, which places poor families into middle-class areas, by using methods of optimal control theory. The underlying premise is that poor families can do better on a variety of social, health, educa-

tion, and economic indicators if they have the opportunity to choose good-quality housing in more-affluent destination communities. The fundamental management question is, how best could such a strategy look like?

**This thesis is organized as follows.** Chapter 2 provides a short overview of the recent problems of segregation in the USA as well as in Europe. The mentioned European countries are England, Germany, Sweden and France. In Chapter 3 the formulation of the mathematical model in terms of a two-state optimal control model is formulated. The following Chapter 4 provides a description of the OCMat toolbox used for the numerical analysis. Chapter 5 discusses the analyses including the investigation of the canonical system, phase portraits and bifurcation diagrams. Finally, cases of indifference are discussed. The thesis closes with a summary, which contains conclusions resulting from the underlying analyses and several policy implications.



## Policy Context

### 2.1 The USA in words and figures

According to the United States Census Bureau (2011b) the number of inhabitants of the US expands every twelve seconds by one person. It makes the United States to the third largest country by population with about 308 million people.

This rather high number of people living in the U.S. is not so much caused by a birthrate but rather by a large-scale immigration from many countries. The birthrate is 30% under the world average, which is still higher than that of most of the European countries. One person immigrates to the country every 43 seconds as per United States Census Bureau (2011b), so the United States are one of the world's most ethnically diverse and multicultural nations.

One of the key problems concerning this kind of expansion is the slow process of assimilation of the immigrants. Social inhomogeneity accompanies unemployment and delinquency and it breeds ethnical segregation followed by urban decay. The United States Census Bureau estimates the number of illegal immigrants at about 11.2 million in 2010. The population growth of Hispanic Americans provides the major demographic trend. Between 2000 and 2008, the country's Hispanic population increased by 32%.

Bernstein and Edwards (2008) claim in their publication "An Older and More Diverse Nation by Midcentury" the following:

"Minorities, now roughly one-third of the U.S. population, are expected to become the majority in 2042, with the nation projected to be 54% minority in 2050. By 2023, minorities will comprise more than half of all children."

The Annual Estimates of the the United States Census Bureau (2011a) provides the following composition of the US population in 2009:

- 79.6% White
- 12.9% African American
- 4.6% Asian American
- 1.0% American Indian and Alaskan Native
- 0.2% Native Hawaiian and Other Pacific Islander
- 1.7% Multiracial

Additionally this study assumes 15.4% of the whole population to be Hispanic<sup>1</sup>, which means 46.9 million people. Hence White Americans are the largest racial group, African Americans are the nation's largest racial minority and Asian Americans are the country's second largest racial minority. Since 1998, China, India, and the Philippines have been in the top four sending countries every year. According to the United States Census Bureau, about 80% of Americans live in urban areas, including suburbs. The "Population Estimates" of the Bureau (2009) specify nine cities with more than one million residents. The biggest metropolises are New York, Los Angeles, Chicago and Houston city with more than two million inhabitants. However, this expansion is associated with large-scale unemployment, where according to the Bureau of Labor Statistics (August, 2011) the average rate amounts to 9.1%. Heavily affected are teenagers by an unemployment of 25.4%, furthermore African Americans by 16.7% and Hispanics by 13.3%, as per the Economic of Labor Statistics (August, 2011). By comparison, as per Die Presse (August 31, 2011), the European Union records an unemployment of 10% with Austria's at 3.7%. The teenager-unemployment in Austria is added up to 7.8%.

Paul Starr (2008)<sup>2</sup> wrote in his article "A New Deal of Their Own" the following:

"America does not do well by its young. [...] In a UNICEF (2007) study last year measuring the well-being of children and adolescents in 21 rich countries, the United States ranked next to last. According to U.S. Census Bureau data, 17% of children in 2006 were growing up in families with incomes below the poverty line – just about the same proportion as in the 1970s. [...] The persistent problems affecting children and the deteriorating economic position of young adults stand in contrast to the historic improvement in the well-being of the elderly during the same period."

---

<sup>1</sup>Hispanic or Latino origin is independent of race and is termed "ethnicity" by the United States Census Bureau. (The racial categories are: American Indian and Alaska Native, White, Black or African American, Asian, Native Hawaiian and Other Pacific Islander.)

<sup>2</sup>Co-editor of the U.S. magazine "American Prospect", which is a biweekly magazine covering politics, culture, and policy from a liberal perspective.

According to DeNavas-Walt et al. (2008) the United States denotes the greatest income inequality among developed nations. This report demonstrates also the varying level of income in different states. Maryland has the highest income added up to \$68,080 and Mississippi the lowest one by \$36,338. Furthermore it sheds light on the American poverty status. In 2008, 13.2% of all Americans lived in poverty, which included more than 30 million people. The harmful effects of high-poverty areas are thought to be especially severe for children whose behavior and prospects may be particularly susceptible to a number of neighborhood characteristics, such as peer group influences, school quality, and the availability of supervised after school activities.

One possibility to reduce destitution is deconcentration of poverty, e.g., via housing mobility programs. By means of dynamic optimization models, this work examines the problem faced by a social planner who wants to integrate poor families into middle-class neighborhoods faced by segregation without inducing “middle-class-flight”<sup>3</sup>.

However, one central question is whether flight is driven more by the current inflow of poor immigrants or by their accumulation over time. On that point, there appears to be some reasons to believe it is the current inflow (Ellen, 2000).

Charles T. Clotfelter<sup>4</sup> is of the opinion, that the Brown v. Board of Education (1954)<sup>5</sup> decision of the Supreme Court - ordering the abrogation of racial segregation of public schools - was and remains the major factor actuating the flight of white Americans from mixed-race communities (Clotfelter, 2004). It is worth to mention, however, that the complexity of problems caused by racial segregation has been a frequently discussed subject at least since the Declaration of Independence, July 4, 1776.

Already, 40 years ago Thomas Schelling<sup>6</sup> has already analyzed this segregative behavior of communities (Schelling, 1971). He showed in his segregation model that a small preference for one’s neighbors to be of the same color could lead to total segregation. He used coins on graph paper to demonstrate his theory by placing pennies and nickels in different patterns on the “board” and then moving them one by one if they were in an “unhappy” situation.

The rule, this model operates on, is that for every colored cell, if greater than 33% of the

---

<sup>3</sup>Middle-class-flight is a demographic and sociological term denoting the trend when middle-class people flee desegregated communities due to anxiety of accustomed social standards.

<sup>4</sup>Professor of Public Policy Studies and Professor of Economics and Law at Duke University.

<sup>5</sup>Supreme Court of the United States: Full name of the case: Oliver Brown et al. v. Board of Education of Topeka et al.

<sup>6</sup>Thomas Crombie Schelling (born April 14, 1921) is an American economist and Professor of Foreign Affairs, National Security, Nuclear Strategy, and Arms Control at the School of Public Policy at University of Maryland, College Park. He received the Nobel Prize in Economic Sciences 2005 “for having enhanced our understanding of conflict and cooperation through game-theory analysis”.

adjacent cells are of a different color, the cell moves to another randomly selected cell. Furthermore, the systemic effects are found to be overwhelming: there is no simple correspondence of individual incentive to collective results. Schelling deduced an “exaggerated separation and patterning result from the dynamics of movement. Inferences about individual motives can usually not be drawn from aggregate patterns” (Schelling, 1971). It is still a powerful example of an “invisible-hand” explanation.

Over the past 10 years the US government has placed an increased emphasis on anti-poverty programs via public housing developments. “The Moving to Opportunity for Fair Housing” (MTO) program directed by HUD (U.S. Department of Housing and Urban Development, 1999) is one of these experimental housing mobility programs (Elhassan et al., 1999). According to the “Moving to Opportunity Interim Impacts Evaluation” Report, MTO was designed to answer questions about what happens when very poor families have the chance to move out of subsidized housing in the poorest neighborhoods of five very large American cities, namely Baltimore, Boston, Chicago, Los Angeles, and New York. MTO was a demonstration program: its unique approach combined tenant-based housing vouchers with location restrictions and housing counseling.

The participant families had to live in public housing or private assisted housing in areas of the central cities with very high poverty rates (40% or more), have very low incomes, and have children under 18 years. The mean poverty rate of baseline locations was, in fact, higher than 56%. The experimental Section 8 group was offered housing vouchers that could only be used in low-poverty neighborhoods (where less than 10% of the population was poor, base year 1990) and local counseling agencies helped to find and lease units in qualifying neighborhoods.

The major questions were: What are the impacts of joining the MTO demonstration on household location and on the housing and neighborhood conditions of the participants? What are the impacts of moving to a low-poverty neighborhood on the employment, income, education, health, and social well-being of family members?

A summary assessment of the findings and the impact estimates suggest that: the findings do provide convincing evidence that MTO had real effects on the lives of participating families in the domain of housing conditions and assistance and on the characteristics of the schools attended by their children; there is no convincing evidence of effects on educational performance, employment and earnings, household income, food security, or self-sufficiency.

However, the ability to measure those effects quantitatively is limited. There are a number of reasons to expect that observing the MTO population over a longer period of time

may reveal significant program impacts in domains with no mid-term effects. There are strong theoretical reasons why it may take many years for the full effects of neighborhood to manifest themselves. Developmental outcomes such as educational performance almost certainly reflect the cumulative experience of the child from an early age. The analyses found at least modest evidence of increasingly favorable effects over time (Elhassan et al., 1999).

## 2.2 Fighting segregation in Europe

This section provides insights into the problem of economical and cultural segregation in Europe. It was already a phenomenon of the middle age's urban development, in as much as merchants and manufacturers lived in different parts of the town. Beside of vocational segregation, an ethnical and religious separation could also be seen in form of the emergence of Jewish Ghettos.

By a rising cultural and ethnical consciousness the issue of segregation became a frequently discussed topic. There are common political attempts to reduce social diversity, with regard to increase social welfare. The high number of scientific studies in the fields of economics, sociology, political science, or Operation Research regarding social segregation shows a significant interest in this topic as well as significant importance. The following pages describe a short excerpt of the variety of numerous scientific investigations.

### Economic Segregation in England: Causes, Consequences, and Policy

The exploration from England carried out by Meen et al. (2005) investigates what makes it difficult to achieve communities with a sustainable mix of incomes and tenures .

Some key findings of their analysis are<sup>7</sup>:

- Patterns of segregation in England have changed little over the past 20 years or more.
- Evidence confirms that 'one-size-fits-all' policies do not work. Different areas need different policies. Areas with very high levels of deprivation need intensive help to reach a 'take-off' point before the private sector is likely to become involved. Otherwise, they become stuck in a poverty trap, segregated from other parts of the community.
- The resources required to reach the take-off point are large in the most deprived areas.

---

<sup>7</sup>read on: <http://www.jrf.org.uk/sites/files/jrf/0645.pdf>, (July 3, 2011, Vienna)

- Segregation and integration depend particularly on where young, high-income households – the most mobile group – choose to move to. Internationally, some of the fastest growing cities have attracted these groups. They are attracted by facilities such as adequate sporting and cultural centres but deterred by areas of high deprivation, unemployment and council taxes. Policies, therefore, have to promote virtuous circles, to avoid the cumulative processes of decline that have been observed historically.
- It is particularly difficult to design policies to attract back older households to cities in order to promote integration, because people tend to move home significantly less as they get older. In general, once households have left urban areas, most tend to stay away.

## **Living and Learning Separately? Ethnic Segregation of School Children in Copenhagen**

Schindler Rangvid (2007) discusses the relation between residential segregation due to ethnical differences and school segregation in Copenhagen<sup>8</sup>.

“The evidence from Copenhagen suggests that low residential segregation does not necessarily translate into moderate school segregation: when school choice options are available (public and, in particular, private), low residential segregation is compatible with high school segregation levels. A decomposition suggests that socioeconomic differences do not seem to be the main driving-force behind school segregation.”

## **Restructuring of Housing and Ethnic Segregation: Recent Developments in Berlin**

Kemper (1998) discusses social segregation caused by a historic event, the fall of the Wall in 1989, followed by massive economical changes in the years of reunification, which were accompanied by a large influx of immigrants. The new immigrants were added to the long-resident guest-worker population settled down in the western part of the city.

“This paper investigates the housing situation of the increasing population of foreigners before and after unification as well as the changing segregation of ethnic minorities. After a comparison of the different housing systems in East and West Berlin and their consequences for ethnic segregation in the 1980s, the main elements of the housing transformation since 1990 are identified and related to the changing residential patterns of foreigners. The patterns of four

---

<sup>8</sup>read on <http://usj.sagepub.com/content/44/7/1329.abstract>, (July 3, 2011, Vienna)

selected nationalities with divergent migration motives are analyzed in more detail. The paper draws attention to differences between East and West Berlin as well as to recent convergences between the two parts of the city.”

## **Public Housing and Residential Segregation of Immigrants in France, 1968-1999**

Following the riots in the suburbs of 2005 in France the media highlighted the consequences of segregation and turned the point of scientific interest tightened in economical and social researches to understand and solve the enduring problem of the evolution of immigrant segregation. Verdugo (2011) documents the large increase in public housing participation rates of non-European immigrants after 1980 and discusses how public housing participation is related to contemporary segregation.

Gaschet and Gaussier (2004) constitute three main reasons to explain the formation of the phenomenon of segregate cities:

“The first one is directly tied to the traditional monocentric model of the New Urban Economics (Fujita, 1989) [...]. Two opposing forces are identified. First, rich households have a high opportunity cost of time and are thus attracted by the accessibility to the city centre. However, as the housing consumption increases with income, rich people are attracted by low prices in the suburbs. The location of richest households thus depends on the evolution of the ratio of the commuting cost to land consumption with income, which can be consistent with a variety of location patterns [...]. The second main approach of urban segregation is a consequence of the preference of households for living in relative homogeneous neighbourhoods in terms of income or ethnic origin (Schelling, 1971) [...]. Thirdly, the occurrence of segregation can be related to housing policies, such as the low apartment’s rents programs intended for low income households. [...]”





# CHAPTER 3

## The Model

The two-state model presented here was first described by Caulkins et al. (1999). While Caulkins et al. (2005a,b) deal with a simplified one-state variant of this model Grass and Tragler (2010) recently studied the full model for the first time. This thesis continues the analysis started in the latter publication.

The model described in what follows is clearly stylized, and many considerations are suppressed in the interest of framing an essential and transparent dynamic of the problem. One key measure of the health of a given neighborhood is taken to be the number of middle-class families who live there at time  $t$ , denoted by the state variable  $X(t)$ . The second state variable  $Y(t)$  represents the number of poor families in the town. With this additional second state variable one can model explicitly the social advancement of marginal families placed by a formal public program into the middle class, with other words the gradual process by which a family remaining in the neighborhood moves up the socio-economic ladder over time. The key policy variable is the rate at which poor families are placed in the neighborhood, denoted by the control variable  $u(t)$ <sup>1</sup>.

The number of middle-class families,  $X$ , varies over time due to three main influences. First, there are the underlying natural or “uncontrolled” dynamics that would pertain even if there were no external intervention (i.e.,  $u \equiv 0$ ). In many respects, housing markets operate like other economic markets, with price adjusting to balance supply and demand and the population converging to some optimal city size (Henderson, 1974), so the housing stock is fixed at a size that would under normal circumstances support some given population (without loss of generality normalized to be unity,  $X = 1$ ). If the resident population grew beyond this normal level ( $X > 1$ ), residents would flow to less congested middle-class neighborhoods. Conversely, if the population falls below that level ( $X < 1$ ), supposably local prices would decline, attracting immigration from other, comparable

---

<sup>1</sup>Note that the time argument  $t$  will mostly be omitted in what follows.

middle-class neighborhoods<sup>2</sup>. To describe this natural adjustment process, the logistic growth curve will be adopted.

The second factor influencing the number of middle-class families is “middle-class flight” induced by the placement of poor families in the neighborhood. The complexity of the incitement of middle-class flight is enormous. Flight may be provoked not only by immigration into the residential neighborhood but rather by immigration of children into the school district (e.g., Clotfelter, 2001; Fairlie, 2002). Some subgroups appear more likely to flee than others. For instance, Ellen (2000) argues that homeowners are more likely to leave than are renters and that families with children are more likely to flee than families without children, particularly if the children attend public schools. Furthermore she explains, “whites do not appear to care very much about the proportion of a neighborhood that is African-American, [but] whites do tend to avoid neighborhoods in which the proportion of families who are African-American is increasing (independent of the current size of the minority population)”. This is akin to the finding of Betts and Fairlie (2003) in the context of native-born and immigrant population that “for every four immigrants who arrive in public high schools, it is estimated that one native student switches to a private school”. The answer to a central question whether flight is driven more by the current inflow of poor immigrants or by their accumulation over time<sup>3</sup> seems to be: the current inflow. So the middle-class flight is assumed to depend primarily as the flow  $u$  of marginal families to the stock of current, established families.

The third and final factor influencing changes in the stock of middle-class residents is the social advancement of poor families, which is the rate at which incoming families are “assimilated”. The hope is that immersion in a middle-class neighborhood will improve outcomes, including labor market participations and income and educational outcomes for the children, which translate into social opportunity and higher incomes over time. However, in accordance with Mayer and Jencks (1989), there is a possibility that affluent neighbors provoke resentment among the poor over their relative deprivation. A satisfying short-term result such as improving social welfare of the neighborhood is almost impractical. Rather, the work is aimed at the long-term benefits as mentioned above.

Summing up the effects influencing the population system, Figure 3.1 illustrates the dynamics of the model.

---

<sup>2</sup>If the population base of the whole city is changing, i.e., if it is booming or eroding, the neighborhood’s normal population density would accordingly change. This analysis assumes the normal population to be constant over time.

<sup>3</sup>Understood relative to the size of the stock of middle-class families.

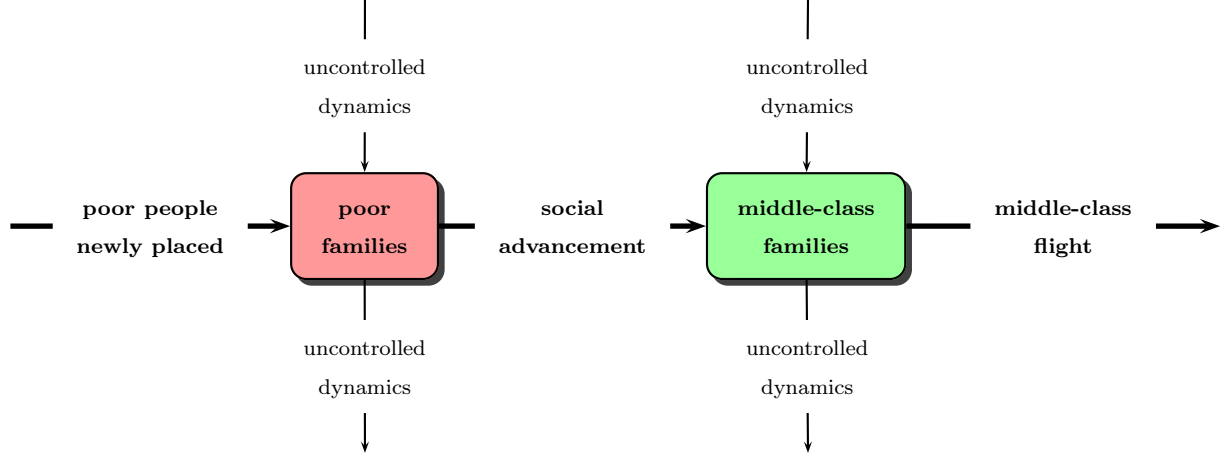


**Figure 3.1:** Placing the poor to the middle-class neighborhood

Together, these considerations suggest the following dynamic optimization problem with two state variables:

$$\begin{aligned}
 & \max_{u(\cdot) \geq 0} \int_0^\infty e^{-rt} [\rho_X X(t) + \rho_Y Y(t) + \sigma(u(t) - cu(t)^2)] dt \\
 & s.t. \quad \dot{X} = \text{own dynamics} - \text{middle-class flight} + \text{social advancement} \\
 & \quad \dot{Y} = \text{own dynamics} - \text{social advancement} + u,
 \end{aligned}$$

where  $r$  is the (non-negative) time discount rate<sup>4</sup>, while  $\rho_X$  and  $\rho_Y$  describe how the decision-maker values directly the presence of established families and of marginal families, respectively. If  $\rho_X = 0$ , then the decision-maker is only concerned about placing as many families as possible. If  $\rho_X > 0$ , then the decision-maker also values directly the presence of established families, e.g., because they pay taxes. Presumably,  $\rho_X > \rho_Y$ ; however, as we will see later, omitting this assumption reveals interesting insights. Further, a weight  $\sigma$  attached to the control terms in the objective function is introduced to allow to put easily more or less emphasis on the contributions from the control variable  $u$  relative to those from the state variables  $X$  and  $Y$ . The control costs are assumed to be quadratic with  $c$  denoting the cost coefficient. What value of parameter  $c$  makes sense is best thought of by leaving aside the  $\rho_X X(t) + \rho_Y Y(t)$  terms, which means by reference only to the instantaneous part of the objective function, which is  $\sigma(u(t) - cu(t)^2)$ , i.e., put the total emphasis on the control. These control terms are maximized when  $u = \frac{1}{2c}$ . A value of  $c = 2$  implies  $u = 0.25$  as the optimal level of the control, which means placing one poor family per four middle-class families per year. Placing one poor family per two middle-class families would be exorbitantly aggressive and would result in less benefit. However, those judgements are probably tempered by long-run considerations including

<sup>4</sup>The time discount rate is a measure of focusing on the future. Obviously, the higher  $r$ , the less is the value of the future, the more important is the present welfare of the society. It is customarily between 3% and 7%, therefore  $r$  is set to 0.05 as base case.

assimilation and middle-class flight. For further details see Caulkins et al. (2005a,b).

A standard way to describe the own dynamics is the logistic growth:

$$\text{own dynamics} = aX(1 - X),$$

where  $X$  is the relative size of the population, and  $a$  ( $b$ , respectively) governs the speed with which the equilibrium population is approached.

The middle-class flight is assumed to be at the form of:

$$\beta f\left(\frac{u}{X}\right) X,$$

where  $\beta$  describes the extent of middle-class flight. Betts and Fairlie (2003) found that one native-born person moved out of the school district for every four immigrants entering ( $\beta = 0.25$ ). Flight by facing lower-class could even be stronger than flight from immigrants, suggesting larger values of  $\beta$ . Ellen (2000) suggests a flight coefficient in the range of  $0.9 - 1.575$ . In light of this, Caulkins et al. (2005a,b) set  $\beta = 0.5$  as base case value. For the increasing function  $f()$  we assume that

$$f\left(\frac{u}{X}\right) = \frac{u}{X}.$$

The social advancement term is assumed to be proportional to  $Y$  with the proportionality factor  $\gamma$ , which is the rate of assimilation of poor families into middle class. Furthermore, it is reasonable to make the social advancement term to be an increasing function of the proportion of neighbors who are middle-class. One of the premises of moving of opportunity programs is that marginal families will learn from their more affluent neighbors and adopt the “successful” practices that lead to middle-class status. So one might imagine that:

$$\text{social advancement} = \gamma Y g(X, Y),$$

with  $g()$  increasing in  $X$ . For instance,

$$g(X, Y) = \left(\frac{kX}{kX + Y}\right)^e,$$

where  $e > 0$ . The constant  $k$  reflects the extent to which the neighborhood was integrated. Therefore,  $k = 1$  describes random mixing, i.e., the proportion of middle-class people to whom a marginal family is exposed is just equal to the proportion of middle class families in the town. If  $k < 1$ , then the proportion of middle-class families seen is less than their factual proportion of the population of the town.

Together, all these reflections suggest the following formulation of the model:

$$\max_{u(\cdot) \geq 0} \int_0^\infty e^{-rt} [\rho_X X(t) + \rho_Y Y(t) + \sigma(u(t) - cu(t)^2)] dt \quad (3.1)$$

subject to the dynamic state equations

$$\dot{X}(t) = aX(t)(1 - X(t)) - \beta u(t) + \gamma Y(t) \left( \frac{kX(t)}{kX(t) + Y(t)} \right)^e \quad (3.2)$$

$$\dot{Y}(t) = bY(t)(d - Y(t)) - \gamma Y(t) \left( \frac{kX(t)}{kX(t) + Y(t)} \right)^e + u(t) \quad (3.3)$$

with base case parameters shown in Table 3.1.

**Table 3.1:** Base case model parameters.

Parameter	Value	Description
$r$	0.05	discount rate
$\rho_X$	0.02	objective function coefficient on $X$
$\rho_Y$	0.01	objective function coefficient on $Y$
$\sigma$	0.01	weight on objective function control terms
$c$	2	program cost coefficient
$a$	2	maximal growth rate at $X = 0$
$b$	2	maximal growth rate at $Y = 0$
$d$	1	carrying capacity of $Y$
$\beta$	0.5	flight coefficient
$\gamma$	0.45	assimilation coefficient
$k$	1	social integration coefficient
$e$	1	exponent in the social advancement term

After describing the model, the next chapter presents the instrument of the analysis, a MATLAB-toolbox called OCMat created by Dieter Grass.



# The MATLAB-Toolbox: OCMat

The OCMat<sup>1</sup> Toolbox initiated by Dieter Grass enables an appropriate analysis of optimal control problems using the MATLAB<sup>®</sup> language<sup>2</sup>. The main emphasis of OCMat is placed on discounted, autonomous, infinite time horizon models though it also provides extensions to non-autonomous, finite time horizon problems. The concentration on this restricted class of optimal control models is well founded as these models are the most commonly investigated problems in economics. The numerical method of the toolbox used to solve optimal control problems is based on Pontryagin's Maximum Principle, which establishes the corresponding canonical system. Essentially, solving optimal control problems is translated to the problem of analyzing the canonical system. In other words, Pontryagin's Maximum Principle defines a boundary value problem (BVP) given by the canonical system, together with the condition for the initial state and some transversality condition<sup>3</sup>.

In addition to the idea of formulating discounted, autonomous, infinite time horizon optimal control models as BVPs, the occurrence of limit sets (equilibria, limit cycles) of the canonical system as long-run optimal solution was the key argument for Dieter Grass to use a continuation method to analyze those BVPs. In general, continuation means continuing an already detected solution while varying a model-specific parameter value. Of course, in the context of a BVP the interest is in the majority of cases not only in continuing a solution for varying model parameters but also in the continuation of a solution along varying initial conditions  $x(0) = x_0$ . Limit sets serve as the first "trivial" solution of an optimal control problem and can be continued in order to derive optimal solutions for

---

<sup>1</sup>OCMat is available via [http://orcos.tuwien.ac.at/research/ocmat\\_software](http://orcos.tuwien.ac.at/research/ocmat_software), (September 20, 2011, Vienna).

<sup>2</sup>MATLAB is a registered trademark of The MathWorks Inc.

<sup>3</sup>For infinite time horizon problems and under the assumption that the optimal solution converges to a limit set, the transversality condition can be replaced by a so-called asymptotic boundary condition. See Grass et al. (2008, Chap. 7.1.4).

arbitrary initial states. The existence of these solutions generated by every continuation step is founded by the implicit function theorem.

One can sum up the main ideas used in OCMat as follows:

- transforming the optimal control problem to a boundary value problem;
- using the technique of continuing an already established solution, which is given by an equilibrium or limit set and
- formulate a so-called asymptotic boundary condition.

More precisely, to introduce the BVP approach, D. Grass starts with the reformulation of an optimal control problem, where it is assumed that the stable manifold of the equilibrium  $(\hat{x}, \hat{\lambda})$  is of dimension  $n$  and is the long-run optimal solution. Then, given an initial state  $x(0) = x_0 \in \mathbb{R}^n$ , a trajectory  $(x(\cdot), \lambda(\cdot))$  has to be found, which satisfies the ODEs of the canonical system and converges to the equilibrium  $(\hat{x}, \hat{\lambda})$  (Grass et al., 2008, p352). Using the definition of local stable manifold this can be formulated so that for some  $T$

$$(x(T), \lambda(T)) \in W_{loc}^S(\hat{x}, \hat{\lambda}),$$

or approximating  $W_{loc}^S(\hat{x}, \hat{\lambda})$  by its linearization  $E^S(\hat{x}, \hat{\lambda})$ ,

$$(x(T), \lambda(T)) \in E^S(\hat{x}, \hat{\lambda}),$$

which provides the terminal condition. Furthermore, the infinite time horizon is replaced by some finite horizon  $T$ . Thus the problem is reduced to a BVP, where initial condition  $x(0) = x_0$  and the terminal condition from above is given.

This short summary of the principles of OCMat presents its key aspects, which serve as the basis for a better understanding of the present work. However, the capacity of the toolbox extends the facility of analyzing two-stage optimal control models quickly, reliably and hence very efficiently, and it also enables the calculation of other problem classes, such as multi-stage models and differential games.

For further information see the OCMat webpage [http://orcos.tuwien.ac.at/research/ocmat\\_software](http://orcos.tuwien.ac.at/research/ocmat_software), which also provides the slides from lectures by Dieter Grass and an OCMat Manual by Dieter Grass and Andrea Seidl. Further details can be found in Grass et al. (2008, Chapter 8)

The next chapter describes the analysis of the underlying discounted, autonomous optimal control model with a specific focus on using OCMat.



# Analysis of the Dynamical System

## 5.1 Introductory analysis

The analysis of the underlying system happens in the usual manner for an optimal dynamic control problem with application of Pontryagin's Maximum Principle (see, e.g., Feichtinger and Hartl, 1986; Grass et al., 2008). It means in its simplest form that the solution of the control problem is delivered from the solution of the so-called canonical system provided by the maximum principle. OCMat is used for the numerical analysis of the system of nonlinear ODEs.

Before the analysis of an optimal control problem with OCMat<sup>1</sup> can be started, some preparing steps have to be done. In particular, a file describing the state dynamics, objective function, and -possibly- control constraint has to be created and initialized. The initializing process consists of two steps: after the creation of the file, MATLAB files containing default information of the model and MATLAB files necessary for the computation have to be generated. For our model, the content of the file has to have the form:

```
statedynamics=sym(' [a*x1*(1-x1)-beta*u1+gamma*x2*(k*x1/
(k*x1+x2))^e;b*x2*(d-x2)-gamma*x2*(k*x1/(k*x1+x2))^e+u1] ');
objectivefunction=sym('sigma*(u1-c*u1^2)+rhox*x1+rhox*x2');
controlconstraint=sym(' [u1-lb] ');
```

where the name of the file is used as the models' name (e.g., BaseCaseModel.m.) `controlconstraint=sym(' [u1-lb] ')` means the control constraint is  $u > 0$ . The file also includes the parameter values. It has to be introduced by the comment `%General`:

```
%General
```

---

<sup>1</sup>For a detailed description, see Grass (2010-2011).

```

r=0.05;
a=2;
b=2;
c=2;
beta=0.5;
gamma=0.45;
e=1;
rhox=0.02;
rhoy=0.01;
d=1;
k=1;
lb=0;
sigma=0.01;

```

The next step is the initialization of the file by

```

initocmat('BaseCaseModel');
m=ocmodel('BaseCaseModel');
files4model(m);
moveocmatfiles(m);

```

`initocmat` derives and stores important information from the `ocmodel`; `ocmodel` constructs an `ocmodel`. The constructor loads the data previously stored during the initialization process. `files4model` creates files for the numerical analysis and `moveocmatfiles` moves the model files from the standard output directory to the standard model directory<sup>2</sup>.

After the initialization process, the analysis of the optimal control problem can be started. It happens in the usual manner, as at first the current-value Hamiltonian is derived, denoted by  $\mathcal{H}$ :

$$\mathcal{H} = \sigma(u - cu^2) + \rho_x X + \rho_y Y + \lambda_1 \left( aX(1 - X) - \beta u_1 + \gamma Y \left( \frac{kX}{kX + Y} \right)^e \right) + \lambda_2 \left( bY(d - Y) - \gamma Y \left( \frac{kX}{kX + Y} \right)^e + u \right).$$

Therefore the toolbox needs at first as always the allocation `m=ocObj`;

With `h=hamiltonian(m)` the Hamiltonian will be dumped. As the Hamiltonian is continuously differentiable in  $u$  with  $u \in \mathbb{R}$ , the Hamiltonian maximizing condition yields

$$\mathcal{H}_u = \sigma - 2c\sigma u - \lambda_1 \beta + \lambda_2 = 0.$$

---

<sup>2</sup>These descriptions can be found at [http://orcos.tuwien.ac.at/fileadmin/t/orcos/OCMat/ocmat\\_lecture1.pdf](http://orcos.tuwien.ac.at/fileadmin/t/orcos/OCMat/ocmat_lecture1.pdf), (September 20, 2011, Vienna).

From the Hamiltonian maximizing condition the optimal control  $u$  can be expressed as:

$$u^* = \frac{\sigma - \lambda_1 \beta + \lambda_2}{2c\sigma}.$$

Using furthermore the costate equation

$$\dot{\lambda}(t) = r\lambda(t) - \mathcal{H}_x,$$

the canonical system in the state-costate-space can be calculated. In principle, the toolbox only needs the command `canonicalsystem(m)` and it displays the general dynamical system using the optimal control  $u^*$ :

$$\begin{aligned}\dot{X} &= aX(1-X) - \frac{\beta}{\sigma c} \left( \frac{1}{2}\sigma - \frac{1}{2}\lambda_1 + \frac{1}{2}\lambda_2 \right) + \gamma Y \left( \frac{kX}{kX+Y} \right)^e, \\ \dot{Y} &= bY(d-Y) - \gamma Y \left( \frac{kX}{kX+Y} \right)^e + \frac{1}{\sigma c} \left( \frac{1}{2}\sigma - \frac{1}{2}\lambda_1 \beta + \frac{1}{2}\lambda_2 \right), \\ \dot{\lambda}_1 &= r\lambda_1 - \rho_X - \lambda_1 \left[ a(1-X) - aX + \gamma Y \left( \frac{kX}{kX+Y} \right)^e e \left( \frac{1}{X} - \frac{k}{(kX+Y)} \right) \right] \\ &\quad + \lambda_2 \gamma Y \left( \frac{kX}{kX+Y} \right)^e e \left( \frac{1}{X} - \frac{k}{(kX+Y)} \right), \\ \dot{\lambda}_2 &= r\lambda_2 - \rho_Y - \lambda_1 \left[ \gamma \left( \frac{kX}{kX+Y} \right)^e - \gamma Y \left( \frac{kX}{kX+Y} \right)^e \frac{e}{kX+Y} \right] \\ &\quad - \lambda_2 \left[ b(d-Y) - bY - \gamma \left( \frac{kX}{kX+Y} \right)^e + \gamma Y \left( \frac{kX}{kX+Y} \right)^e \frac{e}{kX+Y} \right].\end{aligned}$$

The first step of the analysis is to locate the steady states of the canonical system. These are the intersections of the state- and costate-isoclines. For that purpose, command `calcep(m)` is used, with which one can calculate the equilibria analytically, if the system is not too complex. The toolbox also provides the possibility to solve the equations numerically: `rand(4,10)` means in this special case that for the calculation of the equilibrium consisting of four entries (i.e., two states- and two corresponding costate-values:  $X, Y, \lambda_1, \lambda_2$ ) the numerical calculation starts at ten random initial values. The toolbox checks if some solutions are admissible, i.e., they satisfy possible constraints and are actually zeros of the dynamics, with `b=isadmissible(m,ocEP,opt)`. Negativity of state values is checked with `b=isnegativestate(m,ocEP)`. Also repetitive equilibria can be removed by `ocEP=uniqueoc(ocEP,opt)`. With `ocEP{:}` the user gets the calculated set  $(\hat{X}, \hat{Y}, \hat{\lambda}_1, \hat{\lambda}_2)$ . Summing up all these possibilities, the following compound command can be called for calculating the equilibria of the canonical system<sup>3</sup>:

```
ocEP=calcep(m,rand(4,10),opt);b=isadmissible(m,ocEP,opt);ocEP(~b)=[];
b=isnegativestate(m,ocEP);ocEP(b==1)=[];ocEP=uniqueoc(ocEP,opt);ocEP{:}
```

The result is:

---

<sup>3</sup>For setting option, read more on [http://orcos.tuwien.ac.at/fileadmin/t/orcos/OCMat/ocmat\\_lecture1.pdf](http://orcos.tuwien.ac.at/fileadmin/t/orcos/OCMat/ocmat_lecture1.pdf), (September 20, 2011, Vienna), and Grass and Seidl (2008).

ans =

dynprimitive object:

Coordinates:

1.0485

1.0141

0.009113

0.0049762

Arc identifier: 1

Linearization: [4x4 double]

ans =

dynprimitive object:

Coordinates:

0.10486

1.1778

-0.0097546

0.0036071

Arc identifier: 1

Linearization: [4x4 double]

ans =

dynprimitive object:

Coordinates:

1

-1.8606e-010

0.0097561

-0.0095935

Arc identifier: 2

Linearization: [4x4 double]

The first two entries of the column are the state values and the others the corresponding costates of the equilibrium. `Arc identifier` characterizes active or inactive constraints. In particular, 1 refers to an interior solution  $u > 0$ , whereas 2 indicates an equilibrium with an active control constraint.

In what follows, is necessary to consider the equilibria more closely. The third solution can be excluded lying in a non-admissible region. To analyze the first and the second equilibrium, the user can start a continuation process from the state of the first equilibrium into the second equilibrium and vice versa by using:

```
initStruct=initoccont('extremal',m,'initpoint',1,ocEP{1}.dynVar(1,1),
ocEP{2},'IntegrationTime',500);
```

If the continuation processes is successful, the corresponding path is superior and the minor stable path can be excluded.

In the underlying case, the above initialized continuation is successful, i.e., the second equilibrium can be excluded as well. Therefore, only one unique solution exists in the optimal system, namely  $\hat{X} = 1.0485$ ,  $\hat{Y} = 1.0141$ ,  $\hat{\lambda}_1 = 0.009113$  and  $\hat{\lambda}_2 = 0.0049762$ . Finally, the equilibria can be stored by calling `m=store(m,ocEP)`.

To fetch the equilibrium again one has to call `ocEP{1}.dynVar`<sup>4</sup>. To get the Jacobian matrix, the command `J=ocEP{1}.linearization` can be used.

J =

-2.0853	0.1163	6.2500	-12.5000
-0.1088	-2.1725	-12.5000	25.0000
0.0369	-0.0005	2.1353	0.1088
-0.0005	0.0204	-0.1163	2.2225

Moreover, the eigenvalues and eigenvectors of the Jacobian can be displayed by `[eigvec eigval]=eig(ocEP{1})`:

eigvec =

0.4057	0.4253	0.9996	0.7720
-0.8506	-0.8903	-0.0280	-0.6356
-0.2165	-0.0082	-0.0086	-0.0066

---

<sup>4</sup>The class `dynprimitive` represents the “primitive” solutions, equilibria or limit cycles, of the canonical system.

```
-0.2550    -0.1626    0.0000    0.0028
```

```
eigval =
```

```
2.1925      0      0      0
      0  2.3294      0      0
      0      0 -2.1425      0
      0      0      0 -2.2794
```

It exhibits a two-dimensional stable manifold, because the number of eigenvalues  $\xi$  satisfying  $Re\xi < 0$  is two.

The control can be displayed by `u=control(m,ocEP{1})`<sup>5</sup>:

```
u =
```

```
0.2605    0.2605
```

and the value of the Hamiltonian by `h=hamiltonian(m,ocEP{1})`:

```
h =
```

```
0.0324    0.0324
```

Summing up the first results, the underlying model with base case parameter values exhibits four candidates for an optimal solution by solving the canonical system, but only one of them serves as an equilibrium in the optimal system. That means, the system has one unique optimal steady state solution  $(\hat{X}, \hat{Y})$ . The optimal level of middle-class as well as the optimal level of poor families are slightly above the corresponding carrying capacities ( $= 1$ ), with  $\hat{X}$  being insignificantly greater than  $\hat{Y}$  and  $\hat{u}$  being some 4% above 0.25 (cf. Grass and Tragler, 2010).

After this basic analysis of the model, a consideration of the phase portraits will provide deeper insight into the underlying model.

## 5.2 Phase portrait

A phase portrait is used to illustrate the trajectories of a dynamical system in some projection in the state-costate-control space. Phase portraits are an indispensable tool in

---

<sup>5</sup>Since the time grid of an octrajectory consists at least of 0 and 1, the coordinate values of an equilibrium are doubled.

analyzing dynamical systems.

To plot a phase portrait with OCMat at first the user has to set the options that determine the quality and the run-time for the computation of the results<sup>6</sup>. For the calculations described in the present work the following options are recommended:

```
opt=setoptions(opt,'OCCONT','InitStepWidth',0.05/5^4,  
'MaxStepWidth',0.05/5^(0),'MeanIteration',40,'BVP',  
'AbsTol',1e-6,'RelTol',1e-6,'OC','BVPSolver','bvp5c');
```

OCCONT is the main tool for calculating a path with OCMat. It continues an extremal solution (stable path) by solving a BVP<sup>7</sup>. Therefor the BVP-solver `bvp5c` is used<sup>8</sup>. A check of violation of the control restriction is integrated in OCCONT. This facility is important for the calculation of boundary curves and for the continuation of trajectories in an non-admissible interval. By setting the options the user can determinate different increments for a well adapted calculation. For further information see Grass et al. (2008, Chap. 7.2), Grass (2010-2011, Chap. 2.82), and Grass (2010-2011, Chap. 3.125).

The next step is the initialization for the BVP approach. In this case it is done by:

```
initStruct=initoccont('extremal',m,'initpoint',1:2,[0,1],  
ocEP{1},'IntegrationTime',1000)
```

Here INITOCCONT returns the initializing structure for the continuation process, `extremal` describes the continuation type, i.e., an extremal solution is going to be continued. `[0,1]` are the coordinates of the initial state to which the solution is continued. `ocEP{1}` is an initial solution for the analyzed BVP and the `IntegrationTime` denotes for an infinite time horizon model the truncation time. The toolbox solves the BVP by:

```
[sol soln]=occont(m,initStruct,opt);
```

Note that the solution has to be stored at this point by `m=store(m)` to enable the plot. To retrieve a result (already stored in `m`) one can use `ocEP=equilibrium(m)` for retrieving the elements of the fields of the equilibrium and `ocEx=extremalsol(m)` for retrieving the elements of the field according to the stable path. They are stored in `ocResults` among other calculated elements. Note that one can check all the stored calculations made before

---

<sup>6</sup>For more information, see [http://orcos.tuwien.ac.at/fileadmin/t/orcos/OCMat/ocmat\\_lecture2.pdf](http://orcos.tuwien.ac.at/fileadmin/t/orcos/OCMat/ocmat_lecture2.pdf), (September 20, 2011, Vienna), and Grass and Seidl (2008).

<sup>7</sup>As specified above, for the numerical computation at first an initial solution has to be provided which then is continued by OCCONT.

<sup>8</sup>Note that there are different BVP solver for MATLAB.

by calling `m.ocResults`.

After the setting of the necessary options and running the continuation algorithm the user can plot the phase portrait by the following command:

```
clf,type='state';coordinate=2;statecoordinate=1;
plotphaseocresult(m,type,statecoordinate,coordinate,'only',
{'ExtremalSolution'}),hold on,
plotphaseocresult(m,type,statecoordinate,coordinate,'only',
{'Equilibrium'}),hold off, figure(gcf)
```

This command displays the plot of the initialized stable path together with the equilibrium (`'only',{'ExtremalSolution'}`), (`'only',{'Equilibrium'}`) in the phase space, which means the abscissa outlines the first state and the ordinate the second state (`type='state';coordinate=2;statecoordinate=1`). With the command `hold on` or `hold off` the user can choose whether the former plot should be maintained or deleted, respectively.

In the following the process of the above described three steps (initialization, calculation, saving) will be repeated for some other initial points. The chosen initial states are  $[0,1]$ ,  $[2,0]$ ,  $[2,0.5]$ ,  $[0.2,0]$ ,  $[2,1.8]$ ,  $[0.6,2]$ <sup>9</sup>. However, the continuation to the initial point  $[0,1]$  failed and the trajectory ends at the point where it starts to be non-admissible; with other words, this is the point where the control constraint gets violated, i.e., at the boundary between the space with inactive control constraint and active control constraint.

As already noted above, the numerical computation of a stable path using BVP allows the continuation even with a violated control constraint. For this purpose, at first it is necessary to construct a new initial state<sup>10</sup>. The first non-admissible solution serves as the new trivial solution for the continuation. The elements of the field according to the first violated stable path are stored in `extremalsolv(m)`<sup>11</sup>. Now, the user can continue the trajectory from the violation point to the chosen initial point by calling:

```
ocExn=extremalsolv(m);
initStruct=initoccont('extremal',m,'initpoint',1:2,[0,1],ocExn{1});
opt=setocoptions('OCCONT','InitStepWidth',0.01/5^3 , 'MaxStepWidth',12
```

---

<sup>9</sup>The initial points have to be set in `InitStruct` by the initialization.

<sup>10</sup>Reiterating, for the numeric computation an initial solution has to be provided.

<sup>11</sup>Note that the violation has to occur at the first point (see Grass, 2010-2011, Lecture 3)

<sup>12</sup>It is advisable to reduce the `'MaxStepWidth'` and to increase the `'MeanIteration'` compared to the default option setting.



```
0.01,'MeanIteration',50);
[sol soln]=occont(m,initStruct,opt);
m=store(m)
```

and plot it by<sup>13</sup>

```
clf,type='state';coordinate=2;statecoordinate=1;
plotphaseocresult(m,type,statecoordinate,coordinate,
'only',{'ExtremalSolution'},'onlyindex',{[]},'continuous','off',
'limitset','off'),hold on,
plotphaseocresult(m,type,statecoordinate,coordinate,
'only',{'Equilibrium'},'onlyindex',{[]}),hold off,figure(gcf)
```

Notice, the set options are extended by 'continuous', 'off'. It provides a distinguishing in color between the part of the trajectory with inactive and the part with active boundary constraint.

The results of this first analysis are presented in Figure 5.1.

Next, our attention is turned to the boundary curve, i.e., that set of points, where the control constraint gets active. To calculate and plot it the user needs the following commands:

```
initStruct=initoccont('boundary',m,'initpoint',2,0,ocExn{1});14
initStruct=initoccont('boundary',m,'initpoint',2,2,ocExn{1});
opt=setoptions('OCCONT','InitStepWidth',0.01/5^3,'MaxStepWidth',0.01)
m=store(m) [solb solbn]=occont(m,initStruct,opt);

clf,type='state';coordinate=2;statecoordinate=1;
plotphaseocresult(m,type,statecoordinate,coordinate,'only',
{'BoundaryCurve'},'Color',[0 0 0])
```

The continuation is carried out by varying the second coordinate (VARCOORD), while fixing the first coordinate, to zero and then two (VARVAL), set by 'initpoint',2,0 and 'initpoint',2,2. The initial solution is represented by ocExn{1} (OCEXN).

Summing up the descriptions and explanations, the combined commands to plot the phase portrait in 2D or 3D are:

For a 2D plotting use:

---

<sup>13</sup>The plot also contains the equilibrium.

<sup>14</sup>The general command is `initStruct=initoccont('boundary',m,'initpoint',VARCOORD,VARVAL,OCEXN)`.

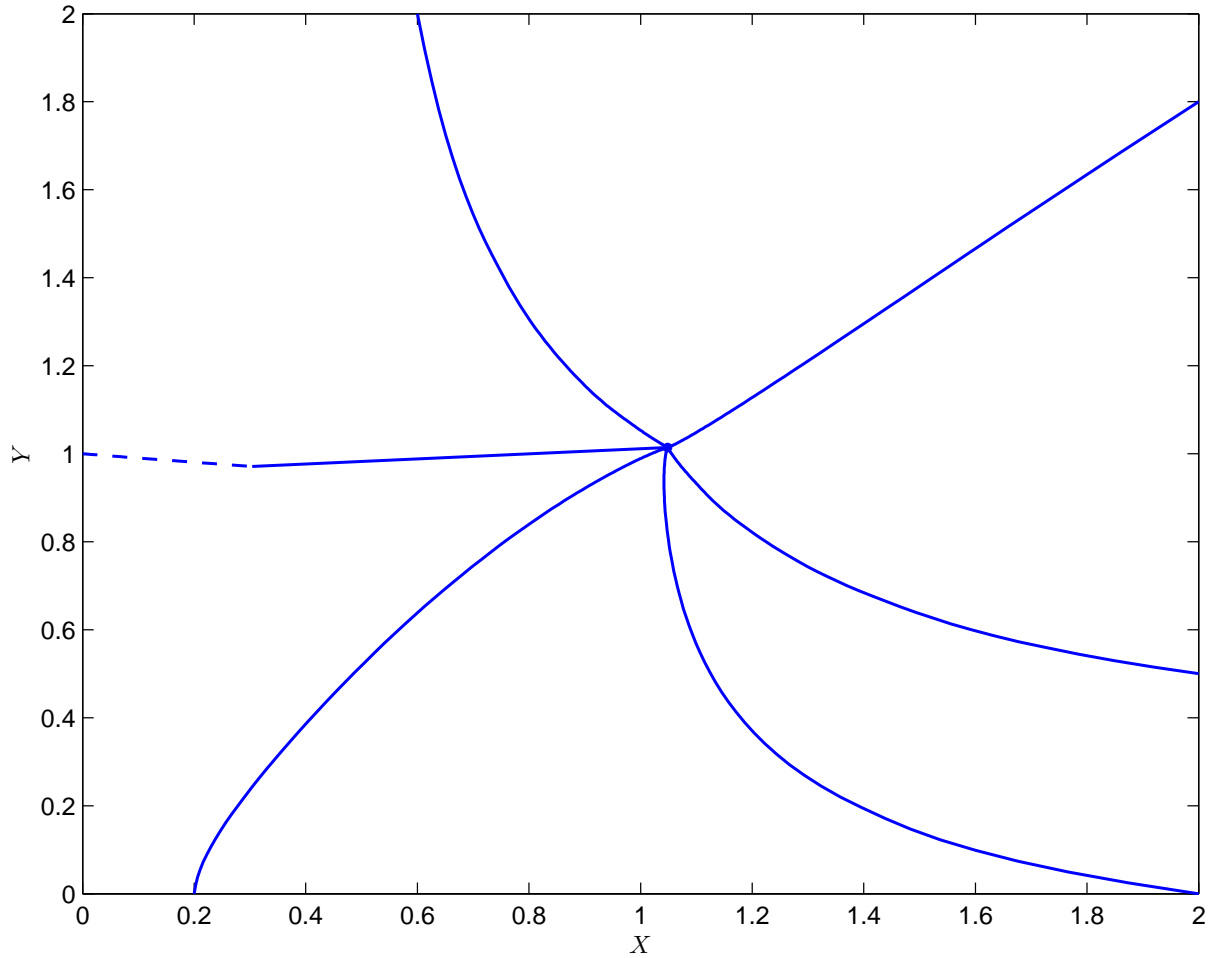


**Figure 5.1:** Phase portrait. The phase portrait depicts six different trajectories in the state space, where  $[1.0485, 1.0141]$  is the equilibrium and the initial states are  $[0, 1]$ ,  $[2, 0]$ ,  $[2, 0.5]$ ,  $[0.2, 0]$ ,  $[2, 1.8]$ ,  $[0.6, 2]$ . The equilibrium is a unique long-run solution of the optimal system. Notice that the control constraint is active at the initial point  $[0, 1]$  (*dashed*).

```
clf,type='state';coordinate=2;statecoordinate=1;
plotphaseocresult(m,type,statecoordinate,coordinate,
'only',{'ExtremalSolution'},'onlyindex',{[]},'continuous','off',
'limitset','off'),hold on,
plotphaseocresult(m,type,statecoordinate,coordinate,
'only',{'BoundaryCurve'},'onlyindex',{[]},'continuous','off',
'Color',[0 0 0]),hold on,
plotphaseocresult(m,type,statecoordinate,coordinate,
'only',{'Equilibrium'},'onlyindex',{[]}),hold off,figure(gcf)
```

For a 3D plotting use:

```
clf,type='control';coordinate=1;statecoordinate1=1;statecoordinate2=2;
```

```

plot3phaseocresult(m,type,statecoordinate1,statecoordinate2,coordinate,
'only',{'ExtremalSolution'},'onlyindex',{[]},'continuous','off',
'limitset','off'),hold on;
plot3phaseocresult(m,type,statecoordinate1,statecoordinate2,coordinate,
'only',{'BoundaryCurve'},'onlyindex',{[]},'associatedsol','off',
'Color',[1 0 0]),
plot3phaseocresult(m,type,statecoordinate1,statecoordinate2,coordinate,
'only',{'Equilibrium'},'onlyindex',{[]}),hold off,figure(gcf)

```

Note that these commands are extended by some applied functions. For example, the limit set of the stable path can be marked by 'limitset','on'. Furthermore it is possible to display only some chosen trajectories which are specified by their indices<sup>15</sup> by setting 'onlyindex'.

The corresponding plotting results are depicted in Figures 5.2 and 5.3.

The analysis of the phase portraits reveals that no control should be applied for a low enough level of middle-class families. This makes economic sense, because when  $X$  is small, both the own growth of the middle-class and its growth due to social advancement are small, so middle-class flight provoked by active governmental control can easily lead to shrinkage of the middle-class in the neighborhood. It is counter-productive both in the short and in the long run (cf. Grass and Tragler, 2010).

The following subsection provides detailed computations on the model by using bifurcation diagrams.

## 5.3 Bifurcation diagrams

In the bifurcation diagram presented in this section we will illustrate the long-term solutions of our optimal control problem by varying single parameters.

The computation of a bifurcation diagram by OCMat bases on calculating the equilibrium while changing a given parameter iteratively. Assuming that small changes of the parameters generate only small changes in the equilibrium values, a Newton method can be used efficiently.

The computation of the bifurcation diagram as a function of any parameter symbolized by `par` on an interval between  $a$  and  $b$  is done by the following command:

```
n=100;parval=linspace(a,b,n)
```

---

<sup>15</sup>For using this function, the command 'gettag' gives a support to find the correct index.

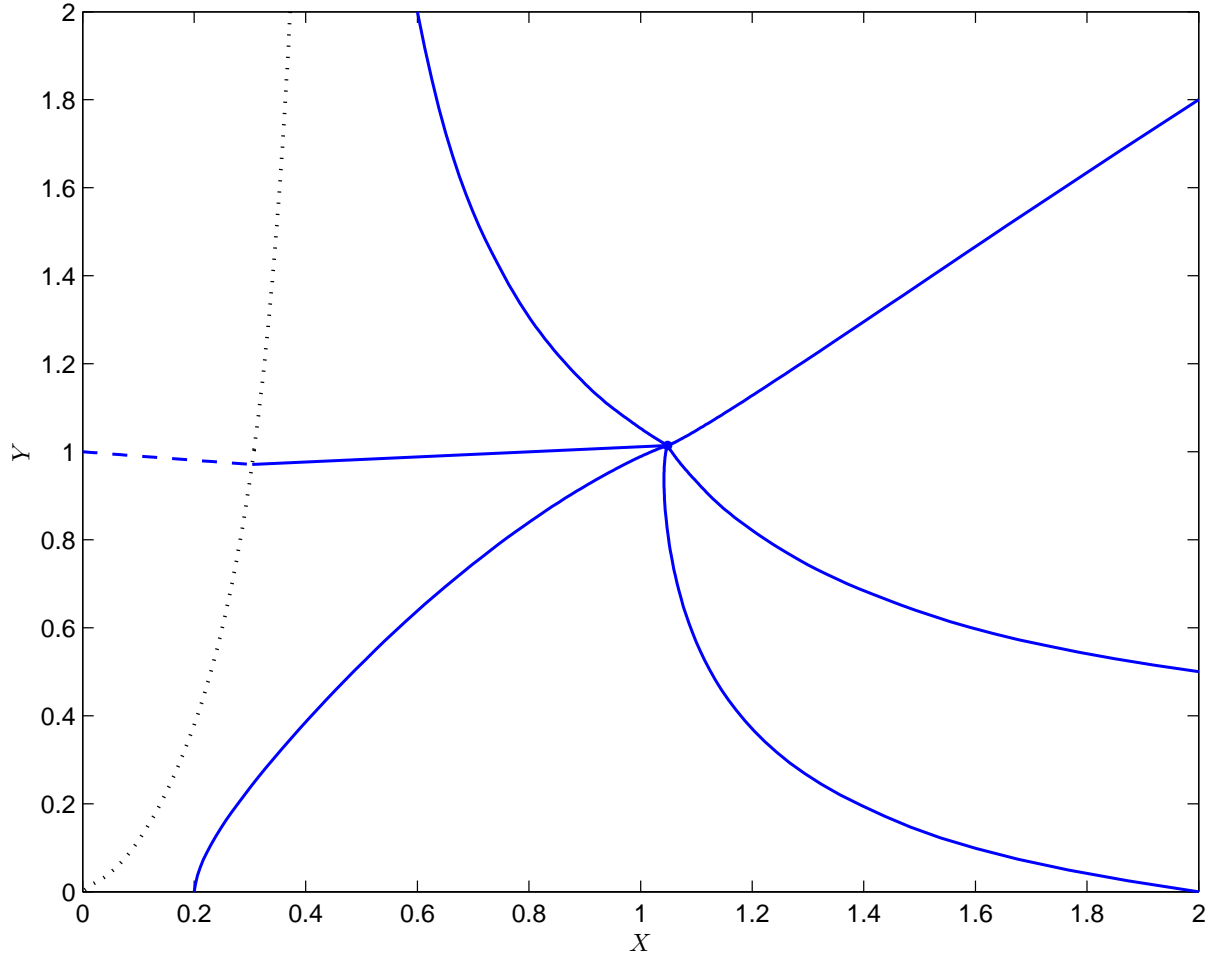


**Figure 5.2:** 2D phase portrait with boundary curve. The phase portrait is an enhancement of Figure 5.1 depicting six trajectories, a unique equilibrium, and the boundary curve (*black dotted*) separating the space with active and inactive control constraint.

```
ocEPinit=ocEP{1};x=[];for ii=1:n; m=changeparameter(m,'par',parval(ii));16
ocEP=calcep(m,ocEPinit.dynVar(:,1),[],1);b(ii)=isadmissible(m,ocEP);
ocEPinitold=ocEPinit;ocEPinit=ocEP{1};x=[x [ocEP{1}.dynVar(:,1);parval(ii)]];
end
```

while 2D or 3D plots are produced by:

```
plot(parval,x(1,:),parval,x(2,:)); or
plot3(parval,x(1,:),u);hold on;plot3(parval,x(2,:),u);
```

First of all, the command contains the vector of the interval with 100 steps on which the parameter moves, followed by setting the initial equilibrium, which has to be continued for the varying parameter. Then the loop for the calculation starts, which is completed

---

<sup>16</sup>ocEP{1} refers to the stored equilibrium.

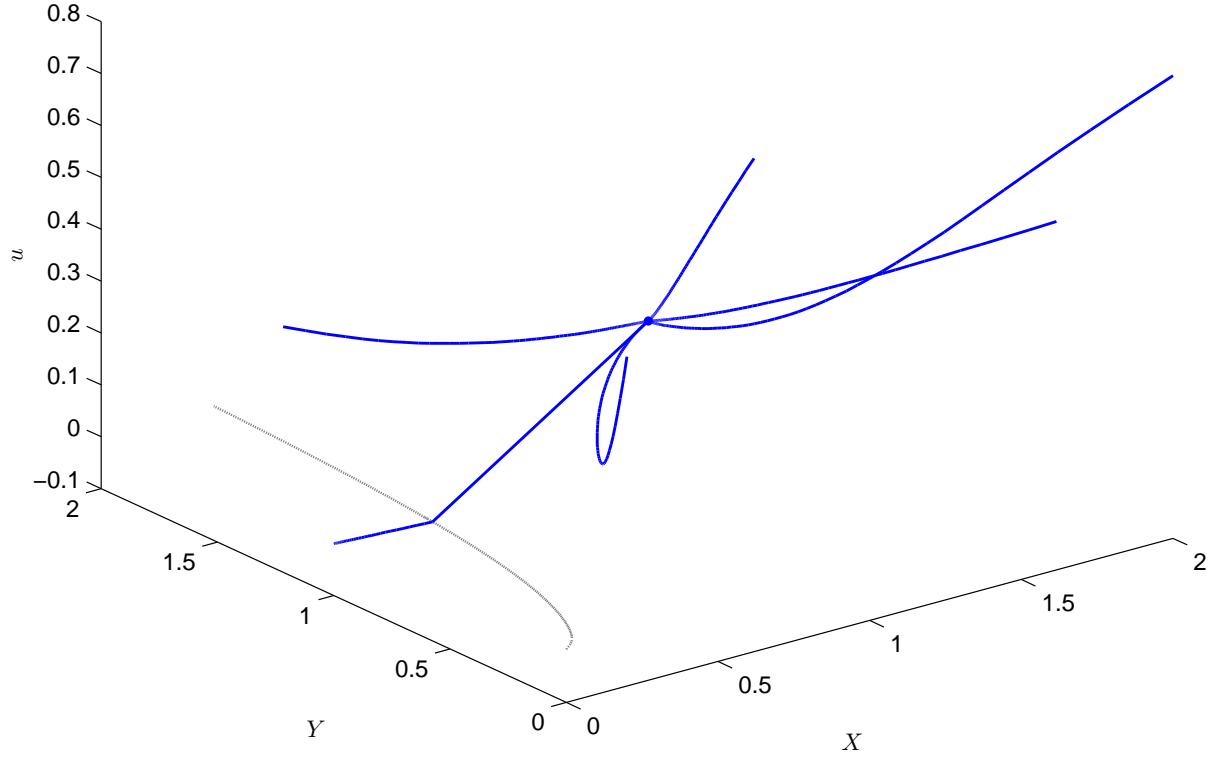


**Figure 5.3:** 3D phase portrait with boundary curve. The phase portrait is a three-dimensional enhancement of Figure 5.2 depicting six trajectories, a unique equilibrium and the boundary curve (*gray*) separating the space with active and inactive control constraint. If the control constraint is active,  $u$  is equal to zero.

by the storage of the calculation.

After this short and general description of the computation of bifurcation diagrams by OCMat, the results for the underlying model considering all parameters will now be presented.

## Discount rate $r$

We start our sensitivity analysis of the system with the discount rate  $r$ . Figure 5.4 describes the behavior of the equilibria varying  $r$  on the interval from 0 to 2.

The non-negative discount rate is a reflection of a society's relative valuation of today's well-being versus the well-being in the future. A large  $r$  means that the future is not highly valued (myopic decision maker), while a small  $r$  represents a strong valuation on the well-being in the future (farsighted decision maker). In general, a small

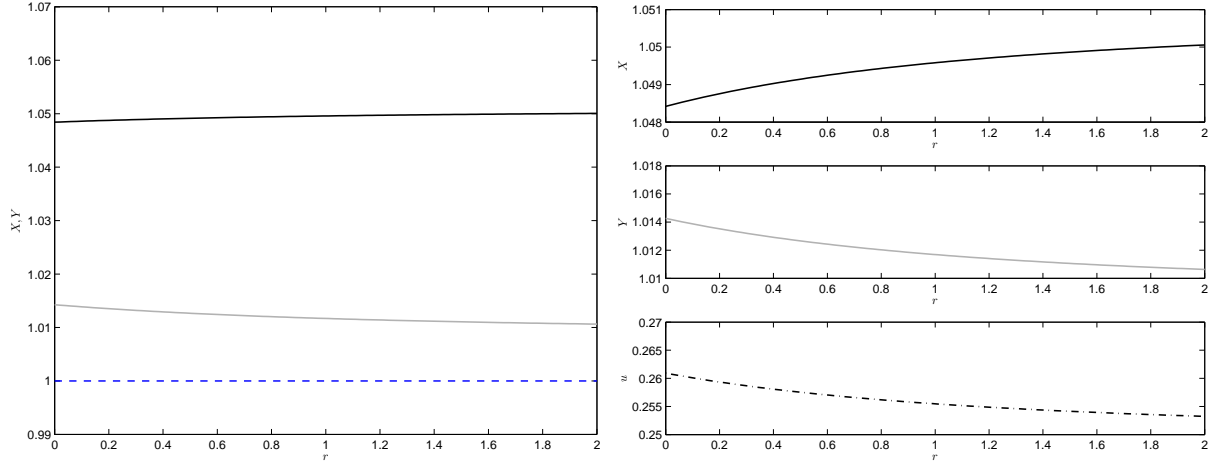


**Figure 5.4:** Discount rate  $r$ .  $X(r)$  (black),  $Y(r)$  (gray),  $u(r)$  (dot-dashed). *Left panel:* optimal population levels of middle-class and poor people for varying  $r$ . Both are above 1, which is the size of the populations under normal circumstances, i.e., in the uncontrolled scenario. *Right panel:*  $X(r)$  is increasing,  $Y(r)$  is decreasing, and  $u(r)$  is as well decreasing.

change in the discount rate can cause significant effects on the benefits derived far in the future, so it is very important to be clear about the choice of  $r$ . See [http://en.wikipedia.org/wiki/Social\\_discount\\_rate](http://en.wikipedia.org/wiki/Social_discount_rate), (6th of January, 2011).

In this sense it is very surprising to find that  $X(r)$  and  $Y(r)$  change only very little for varying  $r$ .  $X(r)$  is a slightly increasing and  $Y(r)$  a slightly decreasing function, but for all practical purposes the system is basically invariant with respect to changes of the discount rate  $r$ . The control  $u(r)$  is as well a decreasing function, but the changes for varying  $r$  are again insignificant in absolute terms.

## Population growth rates $a$ and $b$

The natural population growth is assumed to be purely logistic. The constant  $a$  (resp.,  $b$ ) defines the maximal growth rate at  $X = 0$  (resp.,  $Y = 0$ ). It represents the proportional increase of the population  $X$  (resp.,  $Y$ ) in one unit of time, therefore it can be interpreted as the rate of the housing market adjustment. Later, as the population grows, the second term, i.e.  $-aX^2$  (resp.,  $-bY^2$ ), becomes larger than the first term, which causes an antagonistic effect.<sup>17</sup>

Let  $(b, c, r, k, \beta, \mu, \gamma, \rho_x, \rho_y, \sigma)$  be the set of basic parameters and  $a$  the varying parameter,

<sup>17</sup>see [http://en.wikipedia.org/wiki/Logistic\\_function](http://en.wikipedia.org/wiki/Logistic_function), (2nd of January, 2011)

then the canonical system is given by

$$\begin{aligned}
\dot{X} &= aX(1-X) - \frac{1}{8} + \frac{1}{16}\lambda_1 - \frac{1}{8}\lambda_2 + \frac{9}{20}\frac{XY}{X+Y}, \\
\dot{Y} &= 2Y(1-Y) - \frac{9}{20}\frac{XY}{X+Y} + \frac{1}{4} - \frac{1}{8}\lambda_1 + \frac{1}{4}\lambda_2, \\
\dot{\lambda}_1 &= \frac{1}{20}\lambda_1 - \frac{1}{50} - \lambda_1 \left( a(1-X) - aX + \frac{9}{20}\frac{Y}{X+Y} - \frac{9}{20}\frac{XY}{(X+Y)^2} \right) \\
&\quad - \lambda_2 \left( -\frac{9}{20}\frac{Y}{X+Y} + \frac{9}{20}\frac{XY}{(X+Y)^2} \right), \\
\dot{\lambda}_2 &= \frac{1}{20}\lambda_2 - \frac{1}{100} - \lambda_1 \left( \frac{9}{20}\frac{X}{X+Y} - \frac{9}{20}\frac{XY}{(X+Y)^2} \right) \\
&\quad - \lambda_2 \left( 2 - 4Y - \frac{9}{20}\frac{X}{X+Y} + \frac{9}{20}\frac{XY}{(X+Y)^2} \right).
\end{aligned}$$

If  $b$  is the varying parameter, the canonical system is given by

$$\begin{aligned}
\dot{X} &= 2X(1-X) - \frac{1}{8} + \frac{25}{4}\lambda_1 - \frac{25}{2}\lambda_2 + \frac{9}{20}\frac{XY}{X+Y}, \\
\dot{Y} &= bY(1-Y) - \frac{9}{20}\frac{XY}{X+Y} + \frac{1}{4} - \frac{25}{2}\lambda_1 + 25\lambda_2, \\
\dot{\lambda}_1 &= \frac{1}{20}\lambda_1 - \frac{1}{50} - \lambda_1 \left[ 2 - 4X + \frac{9}{20} \left( \frac{Y}{X+Y} - \frac{XY}{(X+Y)^2} \right) \right] + \\
&\quad \frac{9}{20}\lambda_2 \left( \frac{Y}{X+Y} - \frac{XY}{(X+Y)^2} \right), \\
\dot{\lambda}_2 &= \frac{1}{20}\lambda_2 - \frac{1}{100} - \lambda_1 \left( \frac{9}{20}\frac{X}{X+Y} - \frac{9}{20}\frac{XY}{(X+Y)^2} \right) \\
&\quad - \lambda_2 \left( b(1-Y) - bY - \frac{9}{20}\frac{X}{X+Y} + \frac{9}{20}\frac{XY}{(X+Y)^2} \right).
\end{aligned}$$

The canonical system reveals that  $a = 0$  (resp.,  $b = 0$ ) is not admissible. To calculate  $X$  (resp.,  $Y$ ), a quadratic equation has to be solved. Since  $a$  (resp.,  $b$ ) is the coefficient of the quadratic term, a division by zero occurs in the quadratic formula used to solve the quadratic equation. Therefore, the calculation has to be started slightly away from zero. From a practical point of view, however, this is no restriction, because a zero growth rate does not really make sense anyhow.

The bifurcation diagrams for  $a$  are depicted in Figure 5.5 on an interval beginning at 0.5 and ending at 4. It turns out that  $X(a)$  is a decreasing function and that the optimal level of middle-class families decreases by 20% on the first half of the interval.  $Y(a)$  as well as  $u(a)$  are increasing functions. The higher the growth rate of the middle-class population, the higher the optimal control.

Since  $b$  is the growth rate of  $Y$ , it is now not surprising that  $Y(b)$  is a decreasing function, while  $X(b)$  is increasing, albeit slightly. The higher  $b$ , the lower the optimal

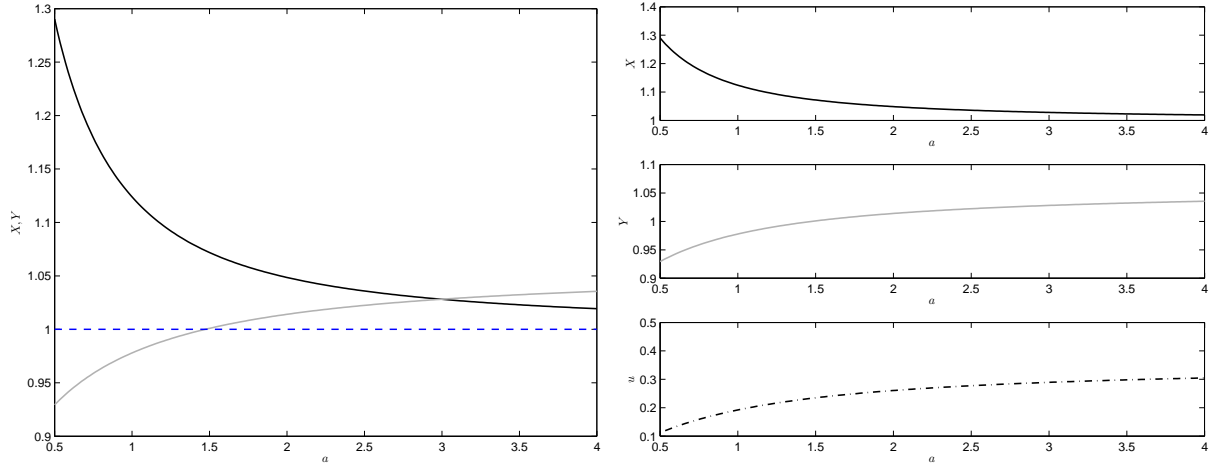


**Figure 5.5:** Maximal growth rate  $a$  at  $X = 0$ .  $X(a)$  (black),  $Y(a)$  (gray),  $u(a)$  (dotted). *Left panel:* optimal population levels of middle-class and poor people for varying  $a$ . The decreasing level of the middle-class population is all along above its baseline size in the uncontrolled scenario. The level of poor families exceeds  $X$  for sufficiently high  $a$ . *Right panel:*  $X(a)$  is decreasing,  $Y(a)$  is increasing, and  $u(a)$  is as well increasing. The control becomes almost constant for sufficiently large  $a$ .

intervention of the decision maker. At the beginning of the interval,  $Y$  exceeds  $X$  significantly, but by increasing  $b$ , the function  $Y(b)$  decreases below  $X(b)$ . See Figure 5.6, which depicts the bifurcation diagram of  $b$  on an interval beginning by 0.5 and ending at 2.

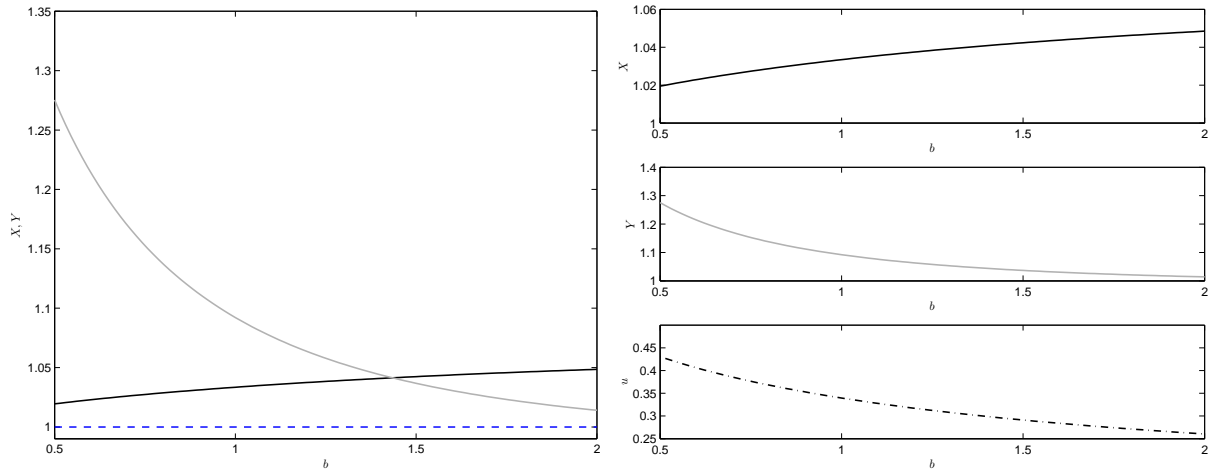


**Figure 5.6:** Maximal growth rate  $b$  at  $Y = 0$ .  $X(b)$  (black),  $Y(b)$  (gray),  $u(b)$  (dotted). *Left panel:* optimal population levels of middle-class and poor people for varying  $b$ . The level of the middle-class population as well as the level of poor people are all along above their baseline size in the uncontrolled scenario. The level of poor families exceeds  $X$  for small  $b$ . *Right panel:*  $X(b)$  is increasing,  $Y(b)$  is decreasing, and  $u(b)$  is as well decreasing.



## Program cost coefficient $c$

This subsection describes the dependence of the equilibria on the program cost coefficient  $c$ . We begin with a short theoretical consideration. Using Pontryagin's Maximum Principle to solve an optimal control problem, one has to consider the Hamiltonian, which yields a unique optimal control value  $u^*$  by

$$\mathcal{H}_u = \sigma - 2c\sigma u - \lambda_1\beta + \lambda_2$$

$$\mathcal{H}_u = 0$$

$$u^* = \frac{\sigma - \lambda_1\beta + \lambda_2}{2c\sigma}$$

It is obvious that  $c = 0$  and  $\sigma = 0$  are parameter values for which a division by zero occurs. Hence, to avoid numerical problems, we exclude those values but start our computations for very small values of  $c$  and  $\sigma$ . Furthermore, considering the canonical system obtained

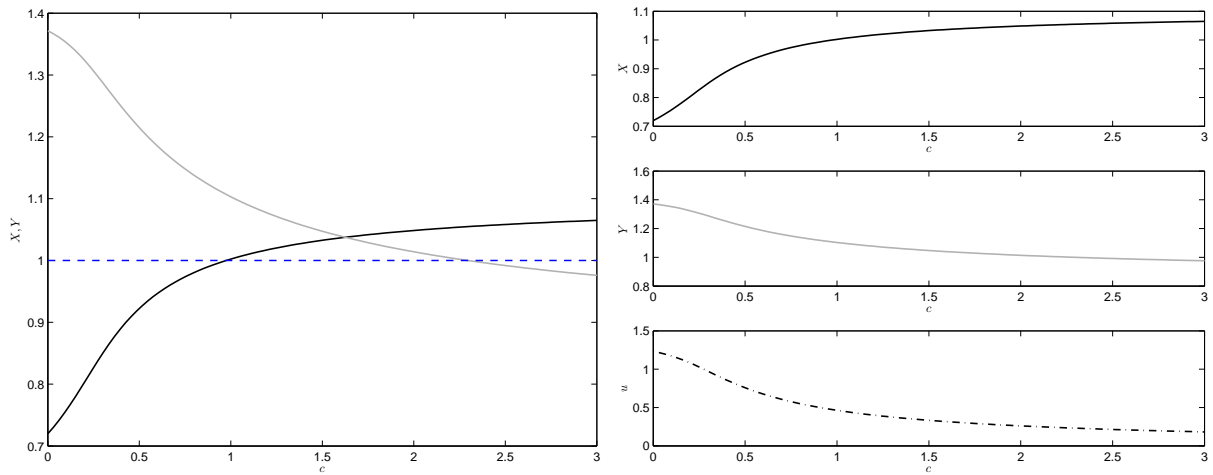


**Figure 5.7:** Program cost coefficient  $c$ .  $X(c)$  (black),  $Y(c)$  (gray),  $u(c)$  (dotted). *Left panel:* optimal population levels of middle-class and poor people for varying  $c$ . As expected, for rising costs the level of middle-class people is increasing while  $Y$  is decreasing as expected. *Right panel:*  $X(c)$  is increasing,  $Y(c)$  is decreasing, and  $u(c)$  is as well decreasing. The decrease in the optimal control is substantial on an interval of  $c$  from 0 to 1, i.e., more than 50%.

for base case parameters varying only  $c$ :

$$\begin{aligned}
\dot{X} &= 2X(1-X) - \frac{1}{c} \left( \frac{1}{4} - \frac{1}{8}\lambda_1 + \frac{1}{4}\lambda_2 \right) + \frac{9}{20} \frac{XY}{X+Y}, \\
\dot{Y} &= 2Y(1-Y) - \frac{9}{20} \frac{XY}{X+Y} + \frac{1}{c} \left( \frac{1}{2} - \frac{1}{4}\lambda_1 + \frac{1}{2}\lambda_2 \right), \\
\dot{\lambda}_1 &= \frac{1}{20}\lambda_1 - \frac{1}{50} - \lambda_1 \left( 2 - 4X + \frac{9}{20} \frac{Y}{X+Y} - \frac{9}{20} \frac{XY}{(X+Y)^2} \right) \\
&\quad - \lambda_2 \left( -\frac{9}{20} \frac{Y}{X+Y} + \frac{9}{20} \frac{XY}{(X+Y)^2} \right), \\
\dot{\lambda}_2 &= \frac{1}{20}\lambda_2 - \frac{1}{100} - \lambda_1 \left( \frac{9}{20} \frac{X}{X+Y} - \frac{9}{20} \frac{XY}{(X+Y)^2} \right) \\
&\quad - \lambda_2 \left( 2 - 4Y - \frac{9}{20} \frac{X}{X+Y} + \frac{9}{20} \frac{XY}{(X+Y)^2} \right),
\end{aligned}$$

reveals that exactly at  $c = 0$  not only for the control function but also for the canonical system a division by zero occurs. Note, however, that for the case  $c = 0$  the quadratic term in the objective function is eliminated, so  $u$  appears only linearly, implying that this hairline case has to be excluded from our analysis based on the assumption of a nonlinear control.

Figures 5.7 and 5.8 show the bifurcation diagrams for  $c$  on different intervals. For low costs, the optimal level of middle-class people is very low. It is not only significantly below the level of marginal families but it is also considerably under the “natural” size in the uncontrolled scenario. In turn, for increasing costs,  $Y$  falls below  $X$ , and even below the natural size at 1.

In summary, the higher the costs the higher  $X$ , and the lower  $Y$  and  $u$ .

## Flight coefficient $\beta$

The following paragraph presents a bifurcation analysis for the flight coefficient  $\beta$ . The corresponding canonical system serves as basis for the numerical computations. It is given

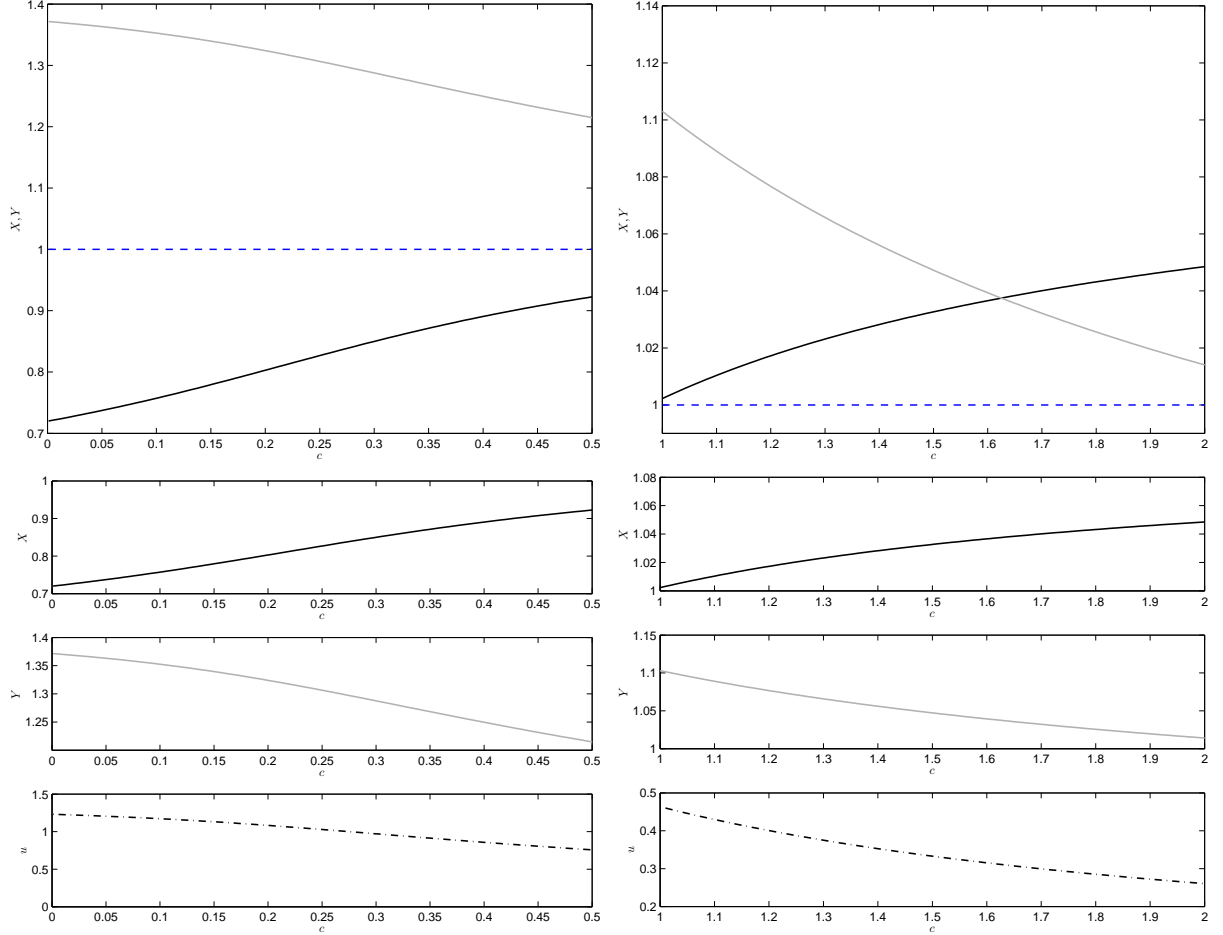


**Figure 5.8:** Program cost coefficient  $c$  on different intervals.  $X(c)$  (black),  $Y(c)$  (gray),  $u(c)$  (dotted). *Top left panel:* For low costs,  $X$  is below its natural size according to normal circumstances (=saturation level), while the level of poor people is considerably high. *Top right panel:* For a cost coefficient between 1 and 2 both the level of middle-class people as well as the level of poor families exceeds the saturation level.  $X$  exceeds  $Y$  at  $c = 1.62$ . *Bottom left panel:* The level of optimal control decreases significantly. *Bottom right panel:* The higher the costs, the smaller the marginal effects on the control term.

by:

$$\begin{aligned}
\dot{X} &= 2X(1-X) - \frac{1}{2}\beta \left( \frac{1}{2} - \frac{1}{3}\lambda_1\beta + \frac{1}{2}\lambda_2 \right) + \frac{9}{20} \frac{XY}{X+Y}, \\
\dot{Y} &= 2Y(1-Y) - \frac{9}{20} \frac{XY}{X+Y} + \frac{1}{4} - \frac{1}{4}\lambda_1\beta + \frac{1}{4}\lambda_2, \\
\dot{\lambda}_1 &= \frac{1}{20}\lambda_1 - \frac{1}{50} - \lambda_1 \left( 2 - 4X + \frac{9}{20} \frac{Y}{X+Y} - \frac{9}{20} \frac{XY}{(X+Y)^2} \right) \\
&\quad - \lambda_2 \left( -\frac{9}{20} \frac{Y}{X+Y} + \frac{9}{20} \frac{XY}{(X+Y)^2} \right), \\
\dot{\lambda}_2 &= \frac{1}{20}\lambda_1 - \frac{1}{100} - \lambda_1 \left( \frac{9}{20} \frac{X}{X+Y} - \frac{9}{20} \frac{XY}{(X+Y)^2} \right) \\
&\quad - \lambda_2 \left( 2 - 4Y - \frac{9}{20} \frac{X}{X+Y} + \frac{9}{20} \frac{XY}{(X+Y)^2} \right).
\end{aligned}$$

The analysis reveals a non-monotonic dependence of  $X$  on  $\beta$ , which is depicted in Figure 5.9. For every value of  $\beta$ , the level of middle-class people is above the saturation level. The minimum of  $X$  is at  $\beta \cong 0.9$ .  $Y(\beta)$  is almost a linearly decreasing function. It even falls below the saturation level. Also the control is a monotonously decreasing function.

It is of particular interest to compare two cases for two different values of  $\beta$  while

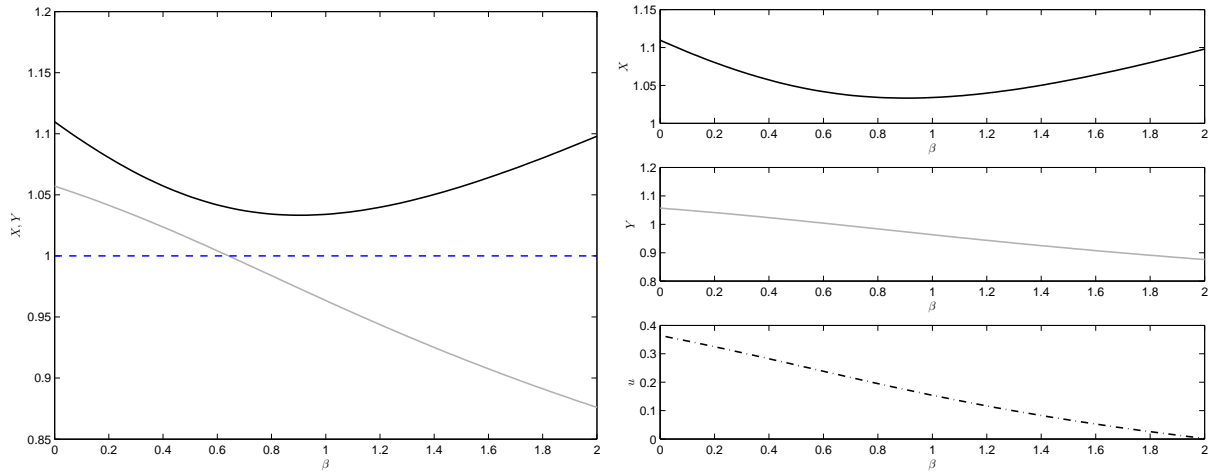


**Figure 5.9:** Flight coefficient  $\beta$ .  $X(\beta)$  (black),  $Y(\beta)$  (gray),  $u(\beta)$  (dot-dashed). *Left panel:* non-monotonicity of  $X$ .  $X$  is all along above its saturation level. *Right panel:*  $X$  is non-monotonic,  $Y$  is almost linearly decreasing, and the control is decreasing, too.

keeping the middle-class families  $X$  at the same level, see Figure 5.10. In case of a very low level of  $\beta$  as well as for a very high one, the number of middle-class families is high. That is a very interesting result, which may best be explained by the corresponding impact on the optimal control  $u$ . It makes sense that the optimal level of the control is decreasing with the flight coefficient, which results in a decreasing level of  $Y$ . Obviously,

when  $\beta$  is very small, the middle-class population can grow best. The worst case in terms of  $X$  occurs at some intermediate level of  $\beta$ , while for even higher values of  $\beta$  the assimilation seems to win over the flight, in particular because control is more moderately used and  $Y$  becomes relatively smaller.

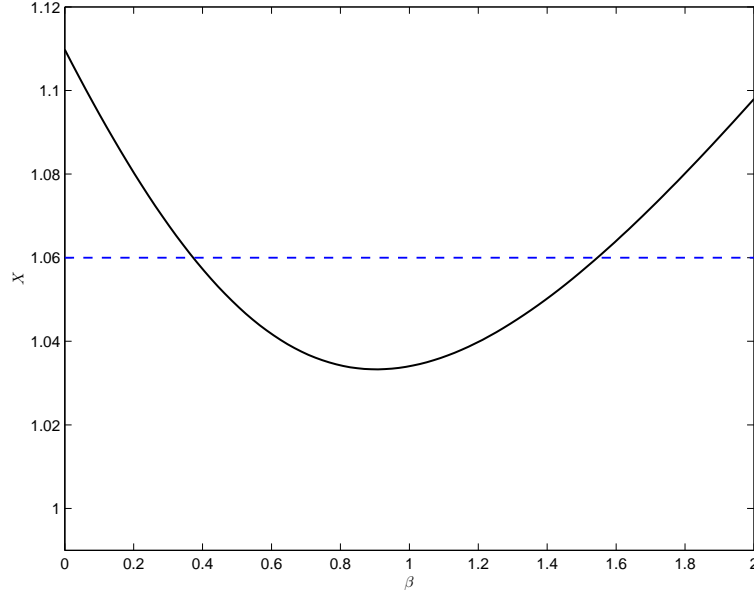


**Figure 5.10:** Non-monotonic dependence of  $X$  on  $\beta$ .  $X(0.374) = X(1.546) = 1.06$ .

The sequence of the phase portraits beginning in Figure 5.11 and ending in Figure 5.16 describes the dynamical change of the equilibrium and the boundary curve by considering some special values of  $\beta$ . Looking at the phase portraits, it is obvious that by increasing the flight coefficient, the region with zero control expands significantly.

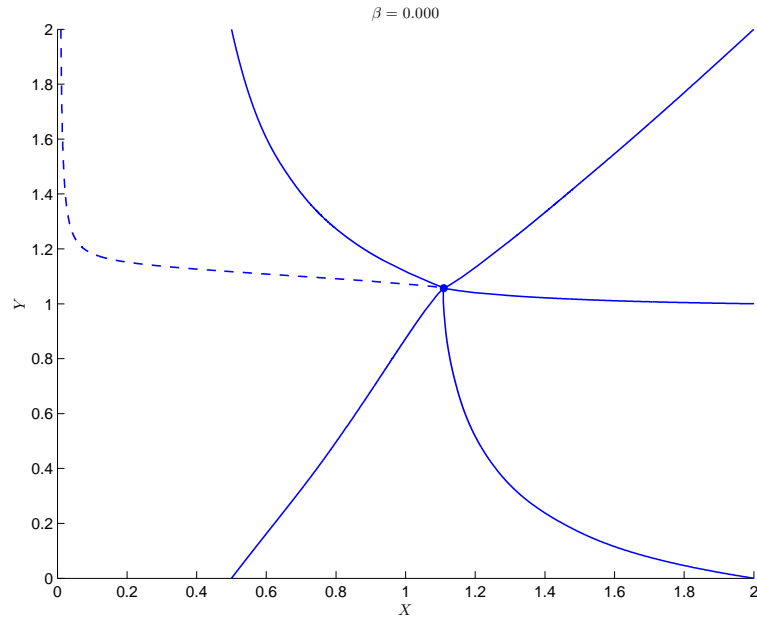


**Figure 5.11:** Left maximum equilibrium level of  $X$  for  $\beta = 0$ .

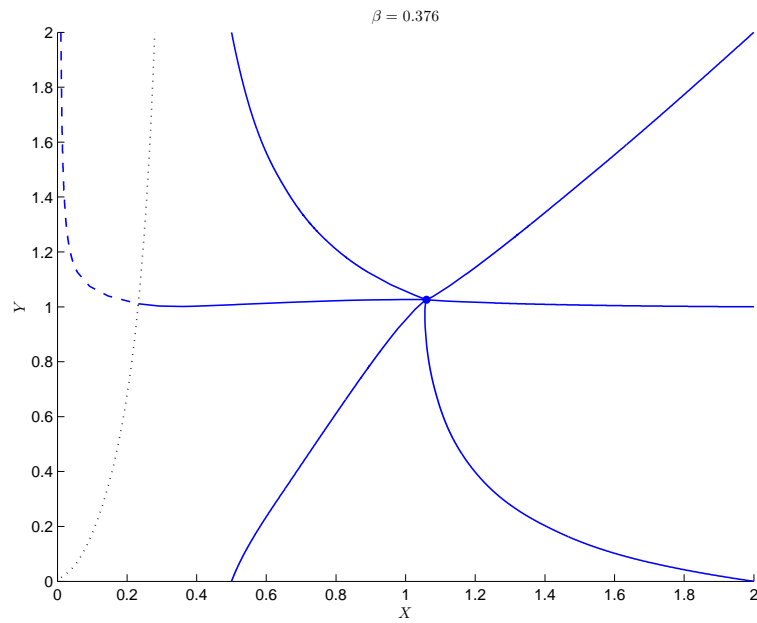


**Figure 5.12:** Equilibrium level of  $X$  at 1.06 for  $\beta = 0.376$  (cf. Figure 5.15).

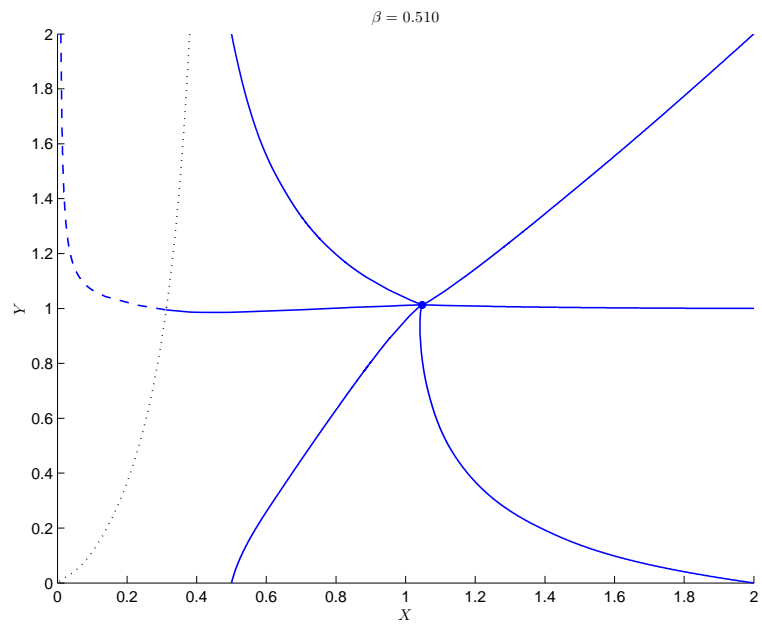


**Figure 5.13:** Base case.

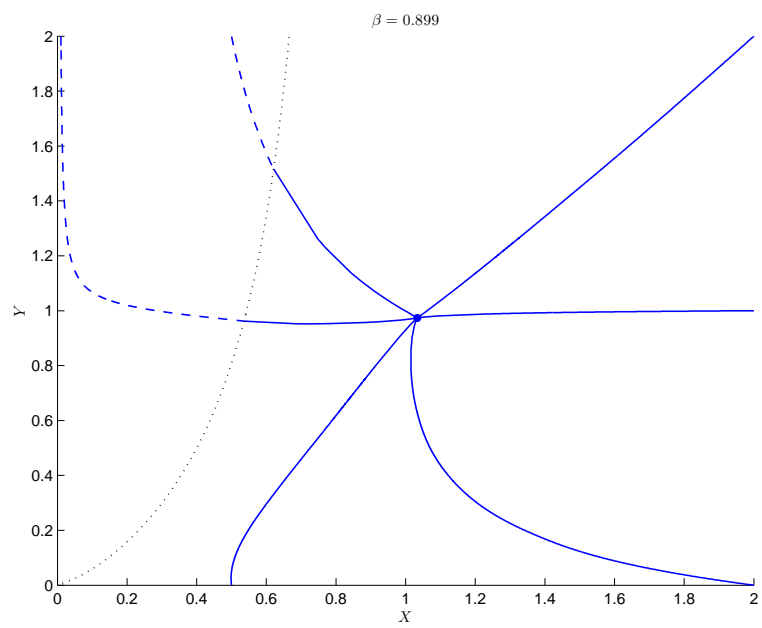


**Figure 5.14:** Minimum equilibrium level of  $X$  for  $\beta = 0.899$ .

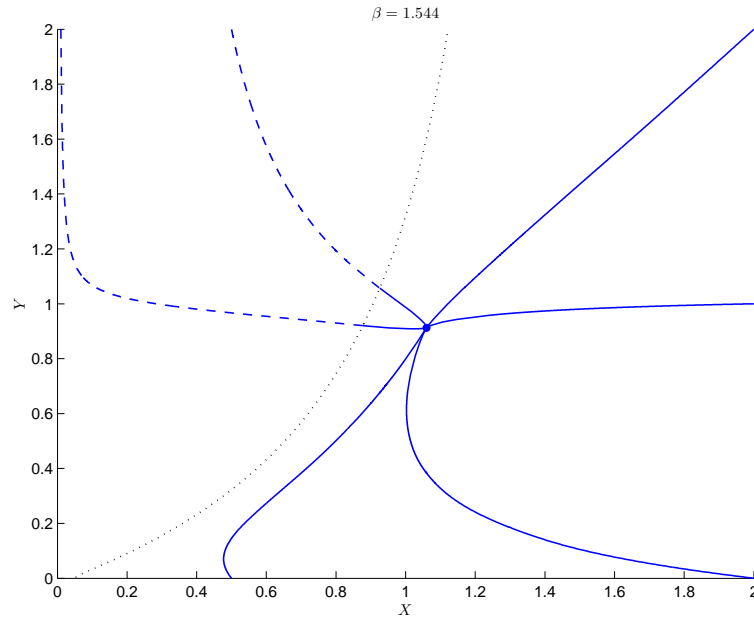


**Figure 5.15:** Equilibrium level of  $X$  at 1.06 for  $\beta = 1.544$  (cf. Figure 5.12).

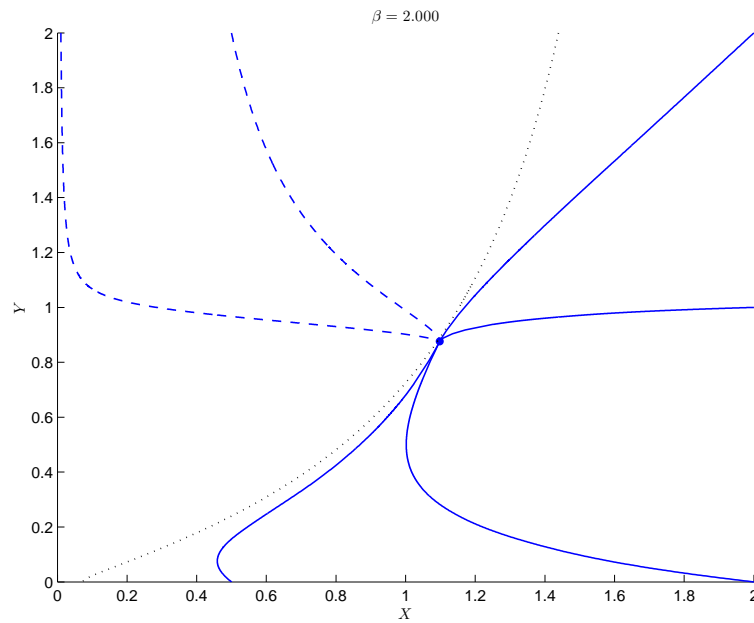


**Figure 5.16:** Right maximum equilibrium level of  $X$  for  $\beta = 2$ .



## Assimilation coefficient $\gamma$

In this subsection we investigate the impact of the assimilation coefficient on the equilibrium levels. It is not surprising that  $Y(\gamma)$  is a decreasing function. The higher the assimilation, the lower the level of poor people. The correlation between  $\gamma$  and  $Y$  is almost linear. If  $\gamma$  is close to zero, the level of middle-class people is below the saturation size. Remarkably, the control  $u$  increases rather moderately with  $\sigma$ . It means the control does not so much depend on the extent of the assimilation of poor people. From an economic point of view, this is an interesting finding.

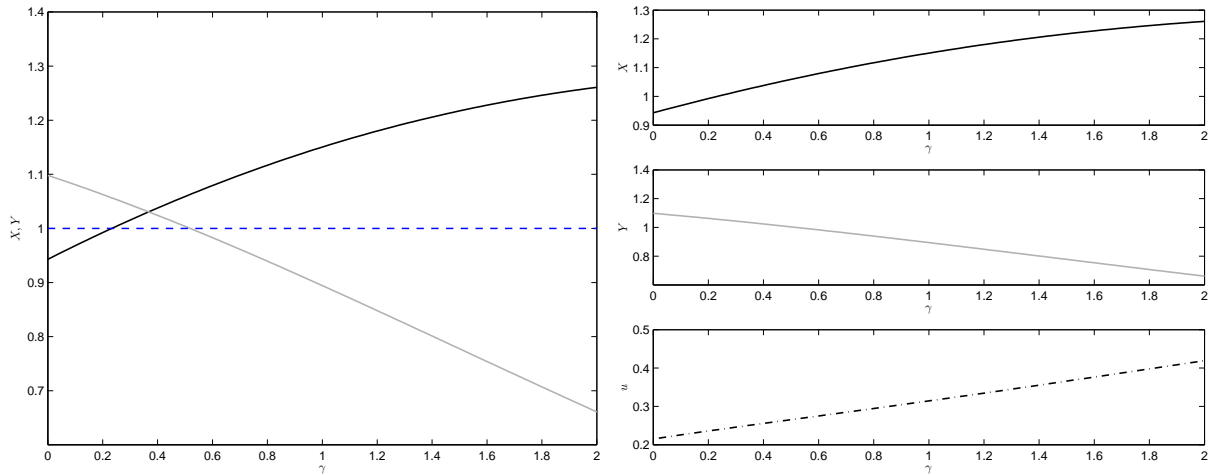


**Figure 5.17:** Assimilation coefficient  $\gamma$ .  $X(\gamma)$  (black),  $Y(\gamma)$  (gray),  $u(\gamma)$  (dotted). *Left panel:* For very low level the assimilation coefficient the level of poor families exceeds the level of middle-class people. *Right panel:*  $X(\gamma)$  is increasing,  $Y(\gamma)$  is decreasing, and  $u(\gamma)$  is increasing.

## Exponent $e$ in the social advancement term

If the exponent in the social advancement term is equal to zero, the advancement term becomes  $\gamma Y(t)$ , that is the maximal extent of the social advancement. For all other positive exponents, the advancement term is smaller. Therefore, for rising  $e$  it is optimal to reduce the control while the level of poor people increases and the number of middle-class people decreases. See Figure 5.18.

## Objective function coefficient $\rho_X$

The following analysis considers the objective function coefficient on  $X$ ,  $\rho_X$  (see Figures 5.19 and 5.20). Not surprisingly,  $X(\rho_X)$  is increasing and  $Y(\rho_X)$  is decreasing. The influence of changing  $\rho_X$  on  $X$  is obviously inverse to the influence on  $Y$ . For very little  $\rho_X$ ,  $Y$  exceeds  $X$ . This is the case when the social benefit is more or less independent of middle-class residents, which most likely would be an unrealistic assumption, interpreting  $\rho_X$  as taxa paid by middle-class people.

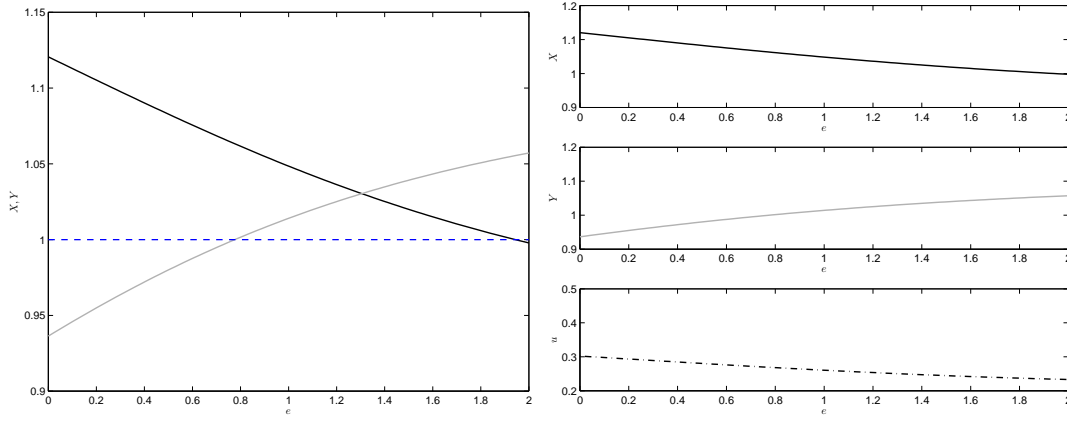


**Figure 5.18:** Exponent in the social advancement term.  $X(e)$  (black),  $Y(e)$  (gray),  $u(e)$  (dotted). *Left panel:* For a sufficiently high exponent  $e$   $Y$  exceeds  $X$ . For a value close to zero, the poor population is under its saturation level. *Right panel:*  $X(e)$  is decreasing,  $Y(e)$  is increasing, and  $u(e)$  is decreasing.

Obviously,  $u(\rho_X)$  is decreasing for every value of  $\rho_X$ . More precisely, for  $\rho_X$  greater than approx. 0.1, the optimal level of  $u$  in equilibrium is even zero. To find out what

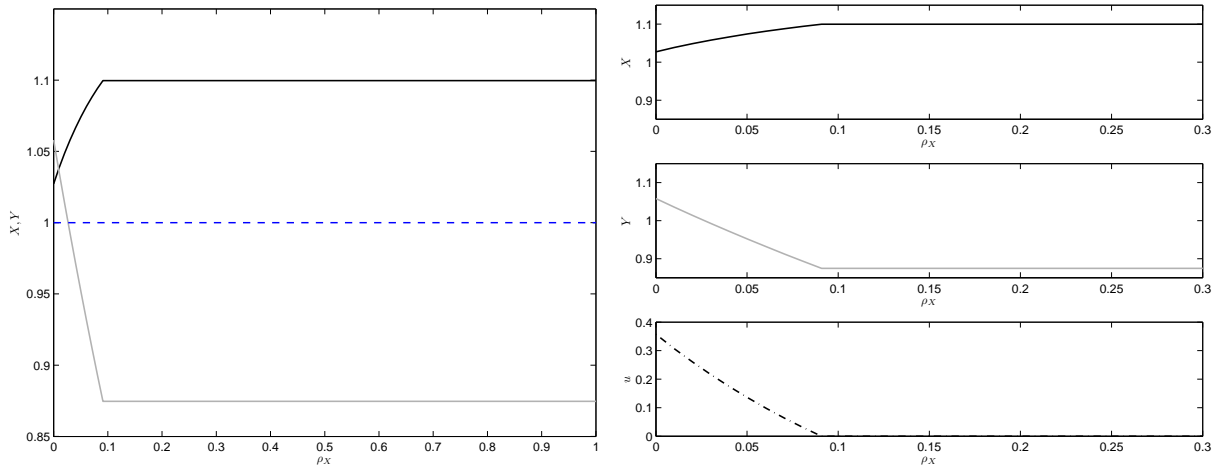


**Figure 5.19:** Objective function coefficient  $\rho_X$ .  $X(\rho_X)$  (black),  $Y(\rho_X)$  (gray),  $u(\rho_X)$  (dotted). *Left panel:* For values of  $\rho_X$  greater than approx. 0.1, it is optimal not to place poor people in the neighborhood. *Right panel:*  $X(\rho_X)$  is increasing,  $Y(\rho_X)$  and  $u(\rho_X)$  are decreasing.

happens for values of  $\rho_X$  close to zero, consider Figure 5.21.

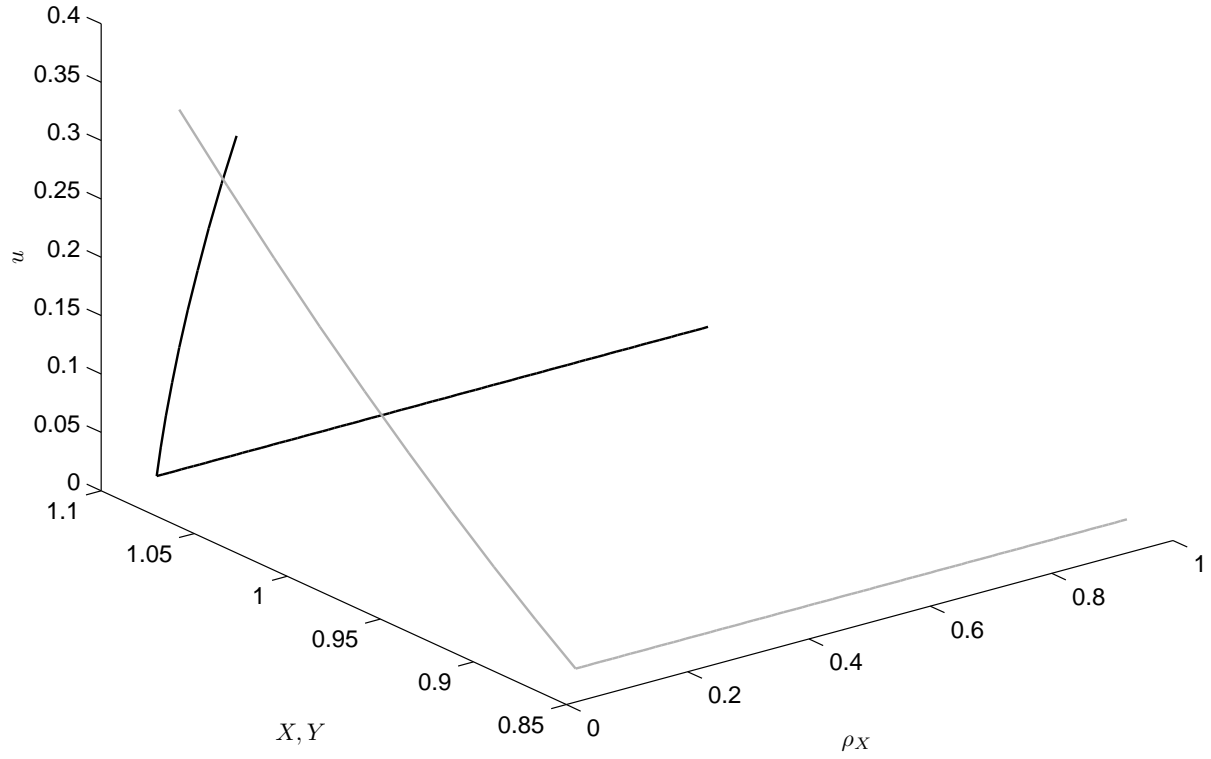


**Figure 5.20:** Objective function coefficient  $\rho_X$  in the state-control space.  $X(\rho_X)$  (*black*),  $Y(\rho_X)$  (*gray*). The strongest effect of  $\rho_X$  on the levels of middle-class families and poor people happens on an interval between zero and approx. 0.1.

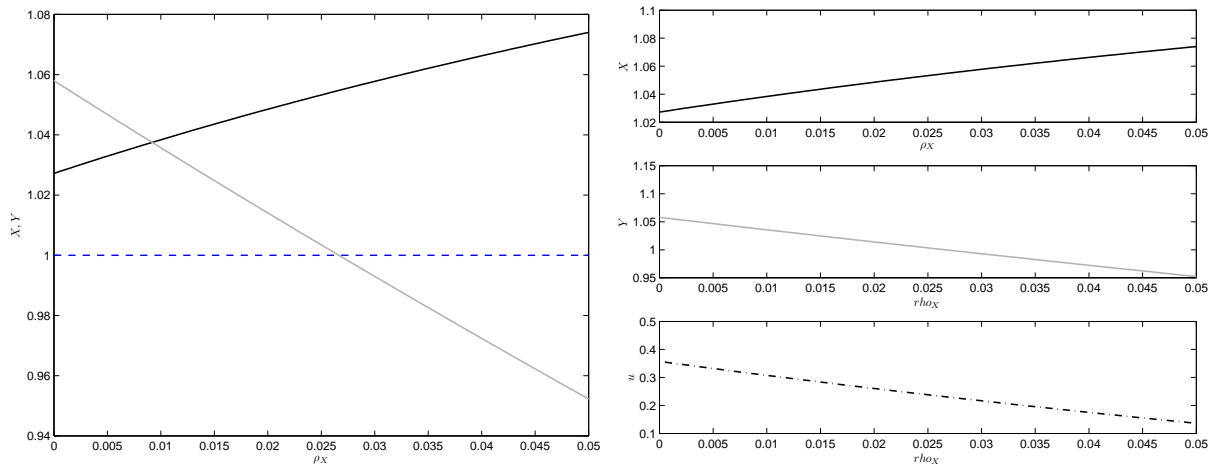


**Figure 5.21:** Objective function coefficient  $\rho_X$ , zoom.  $X(\rho_X)$  (*black*),  $u(\rho_X)$  (*gray*),  $Y(\rho_X)$  (*dotdashed*). *Left panel:* At the very beginning of the interval,  $X$  becomes greater than  $Y$ . *Right panel:*  $u(\rho_X)$  decreases rapidly on the very first section of the interval.

## Objective function coefficient $\rho_Y$

Figures 5.22 and 5.23 depict the bifurcation diagrams for the objective function coefficient on  $Y$ ,  $\rho_Y$ . Interpreting  $\rho_Y$  as a per capita benefit from poor families, it is obvious that with increasing  $\rho_Y$  the number of poor families and the control value increase, which is accompanied by a decreasing level of middle-class families. To get a better picture of the dependence of the equilibrium values on  $\rho_Y$  close to zero, see Figure 5.24. It is highly interesting that both  $u(\rho_Y)$  and  $Y(\rho_Y)$  initially increase significantly, but then saturate quickly at a level of  $\rho_Y$  at approximately 0.2

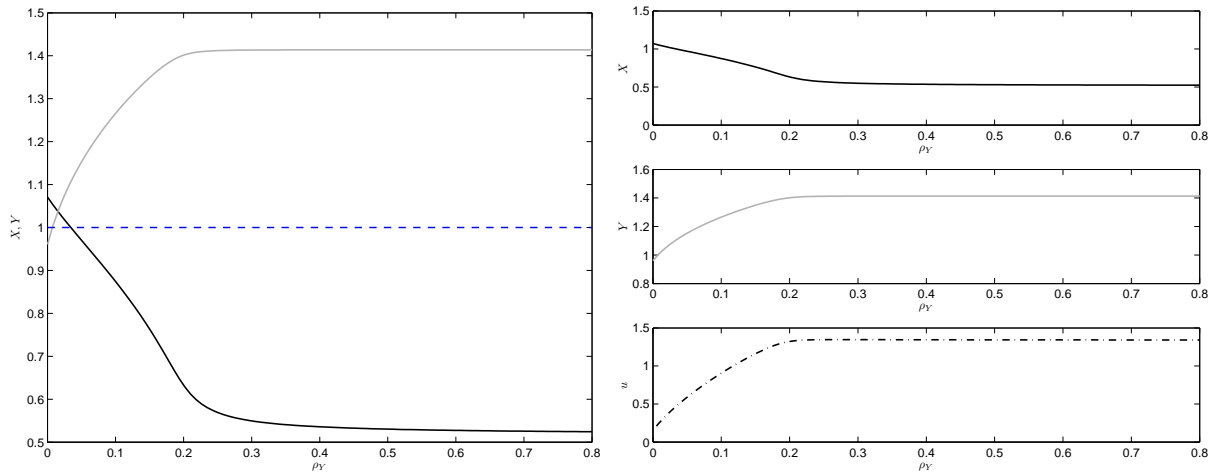


**Figure 5.22:** Objective function coefficient  $\rho_Y$ .  $X(\rho_Y)$  (black),  $Y(\rho_Y)$  (gray),  $u(\rho_Y)$  (dotdashed). *Left panel:* At the very beginning of the interval,  $Y$  surpasses  $X$ . *Right panel:*  $u(\rho_Y)$  increases rapidly on the very first section of the interval, but then saturates quickly.

## Carrying capacity $d$

Next, a short consideration on the carrying capacity of  $Y$ ,  $d$ , is provided (see Figure 5.25).  $d$  denoting the carrying capacity of  $Y$ , it is not surprising that by increasing  $d$ ,  $Y$  as well increases. The correlation between  $d$  and  $Y$  for  $d$  greater than 1 is almost linear which is not surprising neither. However, for  $d$  between 0 and 1,  $Y(d)$  is convex. Moreover, even when the carrying capacity of  $Y$  is zero, the equilibrium level of poor people is above 0.3, which is due to rather high levels of the control. Interestingly,  $X$  is also increasing, albeit moderately. Moreover,  $u(d)$  is concave-convex, but practically decreasing.

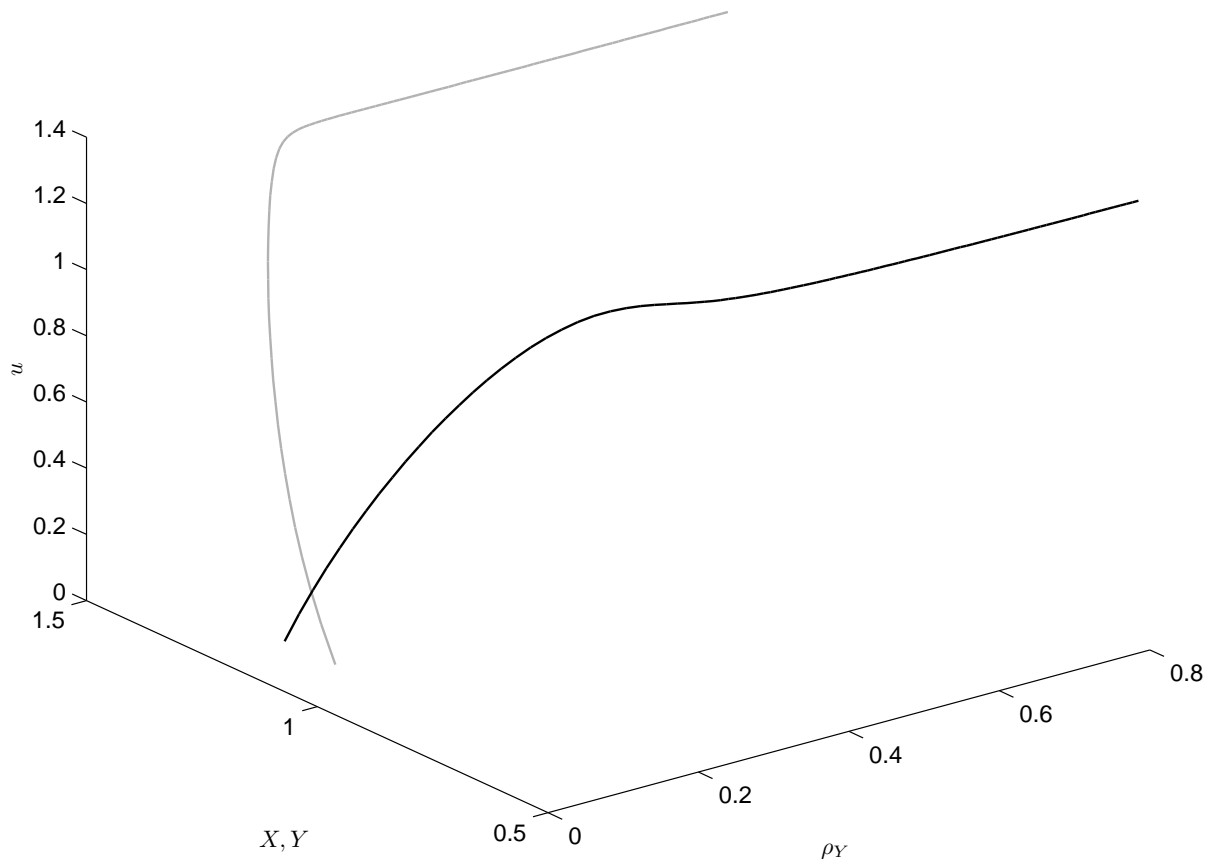


**Figure 5.23:** Objective function coefficient  $\rho_Y$  in the state-control space.  $X(\rho_Y)$  (*black*),  $u(\rho_Y)$  (*gray*). The effect of changing  $\rho_Y$  is the opposite of the effect of changing  $\rho_X$ . The greatest effect of  $\rho_Y$  on the level of middle-class families and on the level of poor people happens on an interval between zero and approx. 0.2.

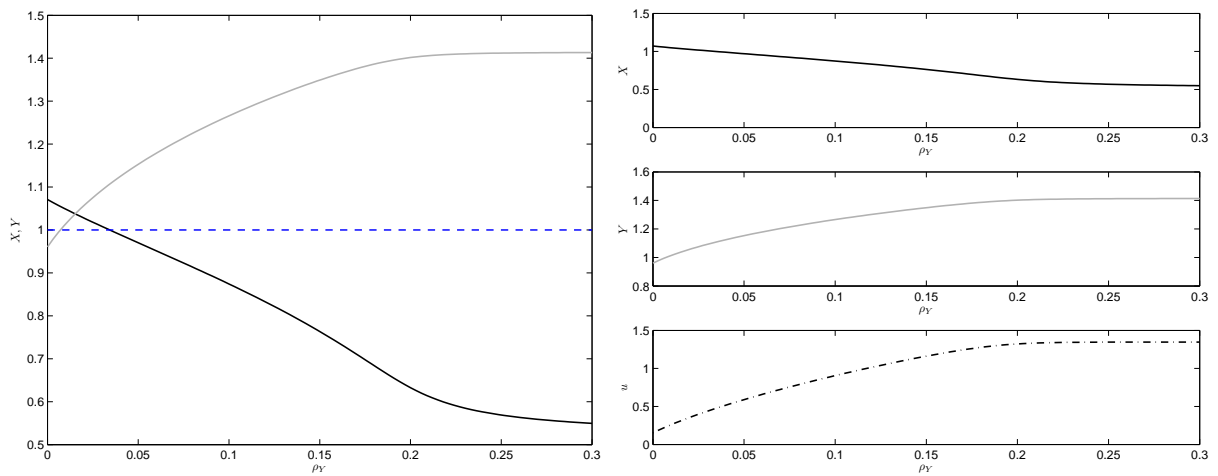


**Figure 5.24:** Objective function coefficient  $\rho_Y$ , zoom.  $X(\rho_Y)$  (*black*),  $Y(\rho_Y)$  (*gray*),  $u(\rho_Y)$  (*dotdashed*).

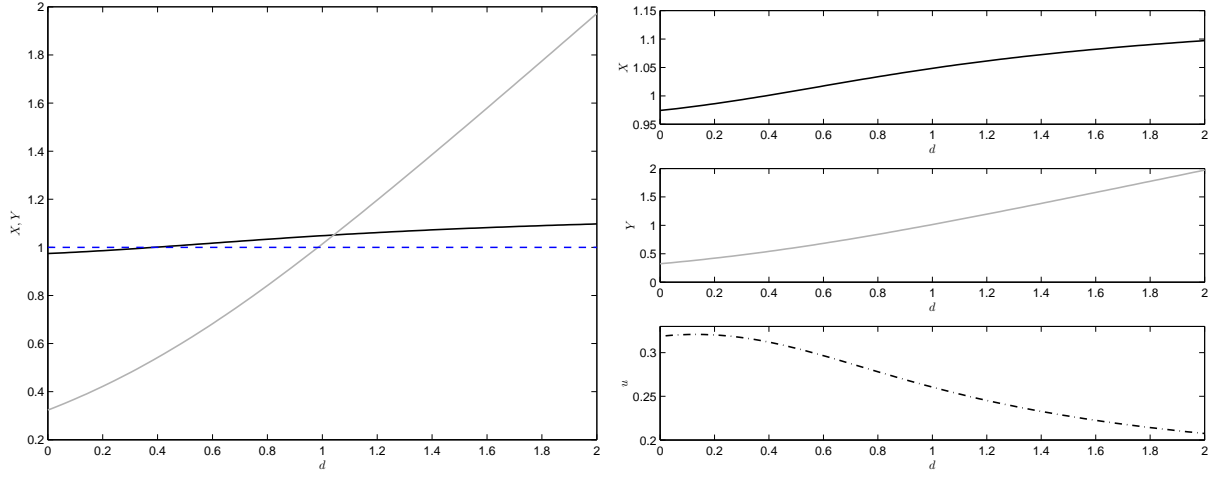


**Figure 5.25:** Carrying capacity  $d$ .  $X(d)$  (black),  $Y(d)$  (gray),  $Y(d)$  (dot-dashed). *Left panel:* The level of  $X(d)$  is slightly increasing but very close to the saturation level.  $Y$  is almost proportional to  $d$ , except for small values of  $d$ , where rather high levels of control compensate for the low saturation level of  $Y$ . *Right panel:*  $X(d)$  increases slightly,  $Y(d)$  increases rapidly, and  $u(d)$  shows a non-monotonic behavior for small  $d$  but otherwise decreases.

## Social integration coefficient

This paragraph describes the bifurcation diagram for the social integration coefficient symbolized by  $k$ , as depicted in Figure 5.26. In general, the impact of the social integration coefficient on the system is very moderate in absolute values. However, the influence is as expected, i.e.,  $X(k)$  is slightly increasing and  $Y(k)$  is slightly decreasing. The level of middle-class people slightly exceeds the natural size. Notably is only the phenomenon that for high value of  $k$   $Y$  falls under its optimal size. Finally, also the control  $u$  increases very moderately.

## Weight $\sigma$ on objective function control terms

This paragraph gives a short consideration on the weight on the objective function control terms,  $\sigma$ , (see Figures 5.27 and 5.28).

The values of  $\sigma$  for which  $X$ ,  $Y$ , and  $u$  are calculated are chosen to be strictly positive. For the hairline case  $\sigma = 0$ , the effect of the control on the objective function is eliminated and our model becomes linear in the control.

This case has to be analyzed individually, which is not considered here.

Our analysis shows that for the chosen set of parameter values,  $\sigma$  has almost no impact on the equilibrium levels of  $u$ ,  $X$ , and  $Y$ .

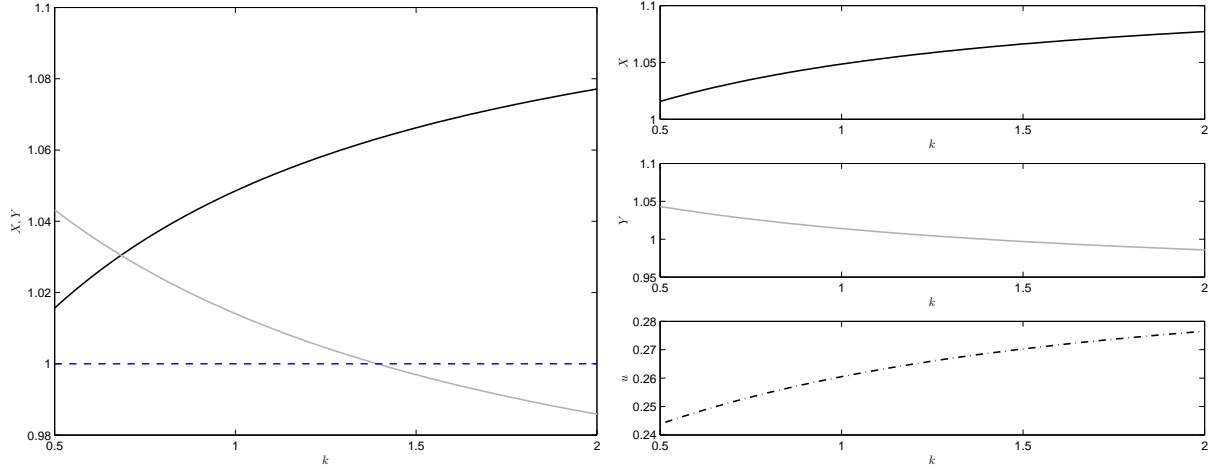


**Figure 5.26:** Social integration coefficient  $k$ .  $X(k)$  (black),  $Y(k)$  (gray),  $u(k)$  (dotted). *Left panel:*  $X(k)$  is above its saturation level and increasing on the whole interval displayed, while  $Y(k)$  is decreasing and eventually falls below its carrying capacity. *Right panel:*  $X(k)$  is increasing,  $Y(k)$  is decreasing, and  $u(k)$  is increasing as well.

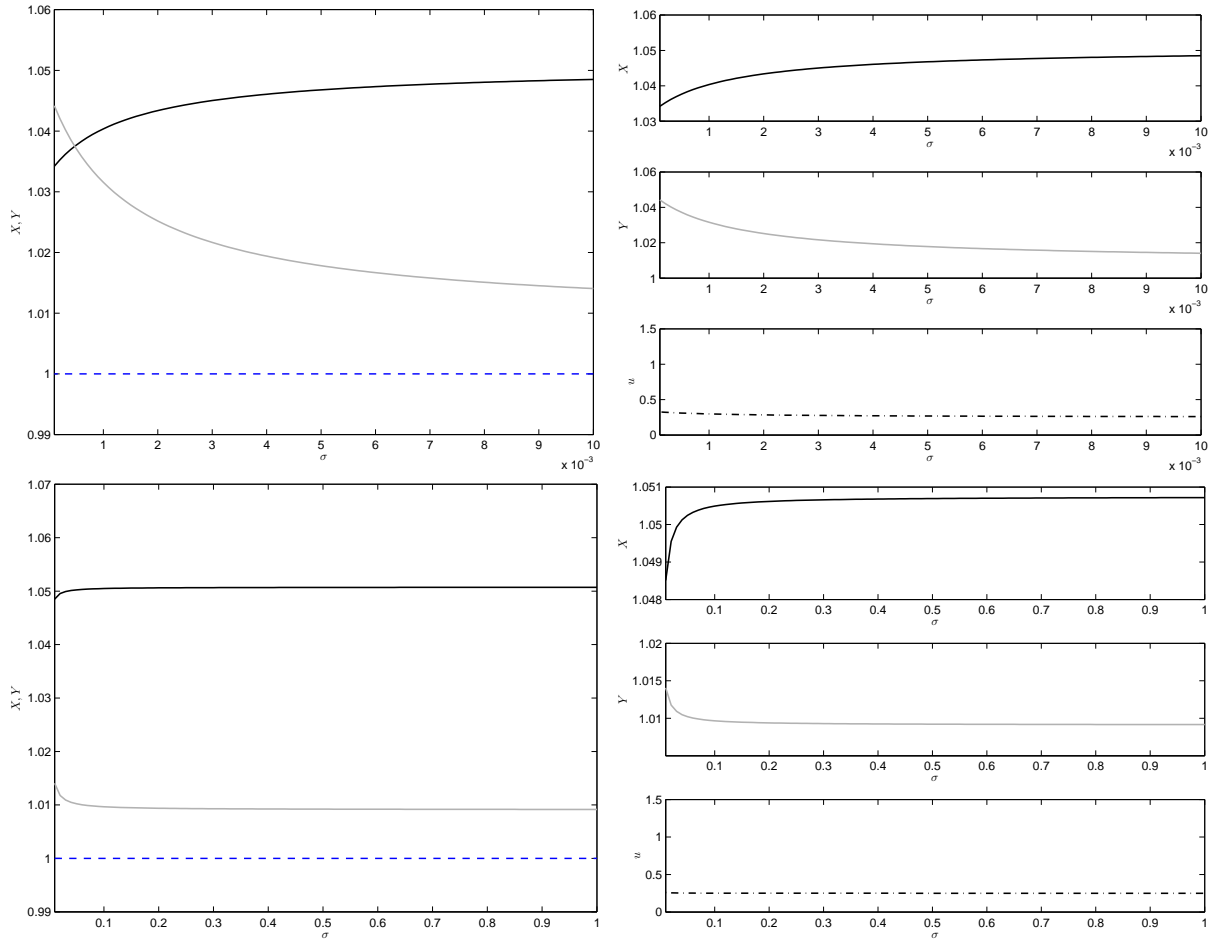


**Figure 5.27:** Weight  $\sigma$  on objective function control terms.  $X(\sigma)$  (black),  $Y(\sigma)$  (gray),  $u(\sigma)$  (dotted). *Left panel:* A change of  $\sigma$  only has an effect at the very beginning of the interval, elsewhere it has no influence. Both  $X$  and  $Y$  are above their saturation level. *Right panel:*  $X(\sigma)$  is increasing,  $Y(\sigma)$  is decreasing, and  $u(d)$  is decreasing.

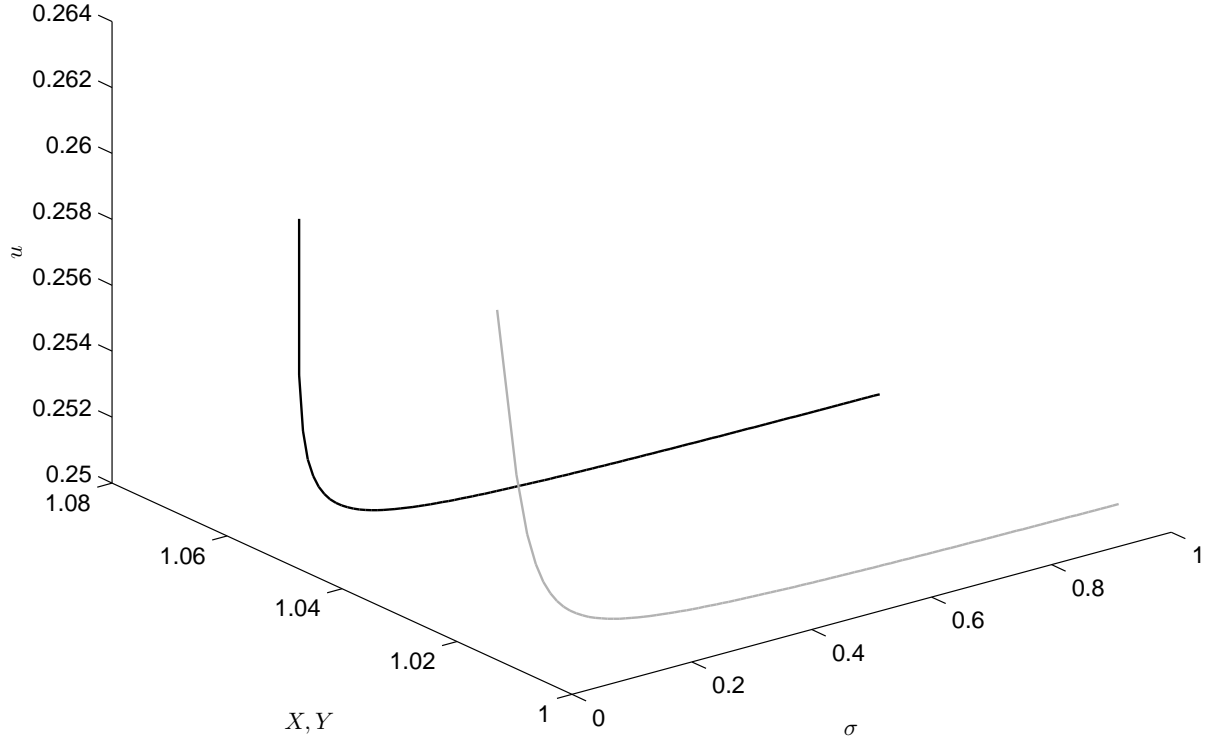


**Figure 5.28:** Weight  $\sigma$  on objective function control terms in the state-control space.  $\sigma(X)$  (*black*),  $\sigma(Y)$  (*gray*). The strongest effect of  $\sigma$  both on  $X$  and on  $Y$  is to be found for low levels of  $\sigma$ .

## Summary

Summing up the bifurcation analysis for the parameters, some interesting observations can be made.

Against expectations, the discount rate  $r$ , i.e., the valuation of today's well-being versus well-being in the future, has almost no influence on the optimal policy, similarly to the weight  $\sigma$  on the objective function control terms, which hardly effects the levels of middle-class people and the level of poor families. On the other hand, different levels of the program cost coefficient cause crucial variations of the equilibrium values. Remarkable is also the non-monotonic case occurring for the level of middle-class by varying the flight coefficient  $\beta$ . Considering the cases of: growth rates ( $a$  and  $b$ ) equal to zero; no cost ( $c$ ); no assimilation ( $\gamma$ ); and no weight ( $\sigma$ ) on the objective function control terms, exhibits non-admissibility, which causes numerical instabilities but is not of practical relevance.

Finally, Table 5.1 summarizes the slopes of the equilibrium values of  $X$ ,  $Y$ , and  $u$  as to be found in the bifurcation diagrams displayed above.



**Table 5.1:** Slopes of equilibria values of  $X$ ,  $Y$ , and  $u$  as functions of the parameters.

Parameter	$X$	$Y$	$u$
$r$	$\nearrow$	$\searrow$	$\searrow$
$a$	$\searrow$	$\nearrow$	$\nearrow$
$b$	$\nearrow$	$\searrow$	$\searrow$
$c$	$\nearrow$	$\searrow$	$\searrow$
$\beta$	$\searrow \nearrow$	$\searrow$	$\searrow$
$\gamma$	$\nearrow$	$\searrow$	$\nearrow$
$e$	$\searrow$	$\nearrow$	$\searrow$
$\rho_X$	$\nearrow$	$\searrow$	$\searrow$
$\rho_Y$	$\searrow$	$\nearrow$	$\nearrow$
$d$	$\nearrow$	$\nearrow$	$\nearrow \searrow$
$k$	$\nearrow$	$\searrow$	$\nearrow$
$\sigma$	$\nearrow$	$\searrow$	$\searrow$

The following subsection discusses the issue of indifference points by analyzing the underlying model for a special set of parameters. As the analysis was carried out again by OCMat toolbox, the way of computing indifference points with the toolbox will as well be subject of the following description.

## 5.4 Indifference points

Multiplicity means that for a given initial state there exist multiple optimal solutions. The set of initial points where the decision-maker is indifferent about which optimal solution to choose are called points of indifference. Note that indifference points are also denoted as Skiba points or DNS(S) points in the related literature. At such a point, at least two different optimal policies exist. However, only a small movement away from such an indifference point provides a unique optimal path (see Grass et al., 2008, Chap. 5). Summing up, the main properties that an indifference point has to satisfy are multiplicity and separability. In contrast, so-called “weak” Skiba points only satisfy the property of separability.

In what follows, a case of indifference will be presented. Note that for this analysis the set of parameters are specified as summarized in Table 5.2 (cf. Grass and Tragler, 2010, Sec. 4.1). Table 5.3 highlights those parameters that differ from the base case. Here

**Table 5.2:** Parameter set exhibiting indifference points.

Parameter	Value	Description
$r$	<b>1</b>	discount rate
$\rho_X$	<b>0</b>	objective function coefficient on $X$
$\rho_Y$	<b>2</b>	objective function coefficient on $Y$
$\sigma$	<b>1</b>	weight on objective function control terms
$c$	<b>1</b>	program cost coefficient
$a$	2	maximal growth rate at $X = 0$
$b$	2	maximal growth rate at $Y = 0$
$d$	1	carrying capacity of $Y$
$\beta$	0.5	flight coefficient
$\gamma$	<b>0.5</b>	assimilation coefficient
$k$	1	social integration coefficient
$e$	1	exponent in the social advancement term

**Table 5.3:** Comparison of parameter values on base case vs. indifference case.

Modified parameter	Base case value	Indifference case value
$r$	0.05	1
$\rho_X$	0.02	0
$\rho_Y$	0.01	2
$\sigma$	0.01	1
$c$	2	1
$\gamma$	0.45	0.5

we assume that the discount rate is abnormally high. Furthermore, only poor families are assumed to contribute to the social benefits, which means that the model ignores the importance of positive social effects caused by middle-class people such as paying taxes.

However, the investigation of such a case gives interesting methodological insight into the application of optimal control theory.

Figure 5.29 depicts the indifference curve in the state space together with some trajectories, which point out the meaning of indifference and also characterize the flow of the optimal vector field. It also shows the boundary curve with a trajectory starting in an area with  $u = 0$ . The indifference curve separates two equilibria with a similar level of poor families but a low versus high level of middle-class people, respectively. Starting at any point of the indifference curve, the decision-maker has two options, i.e., choosing the left or the right solution. Given the vertical shape of the indifference curve, the long-run outcome primarily depends on the initial value of  $X$ .

In both steady states,  $Y$  is larger than its carrying capacity, which is not surprising

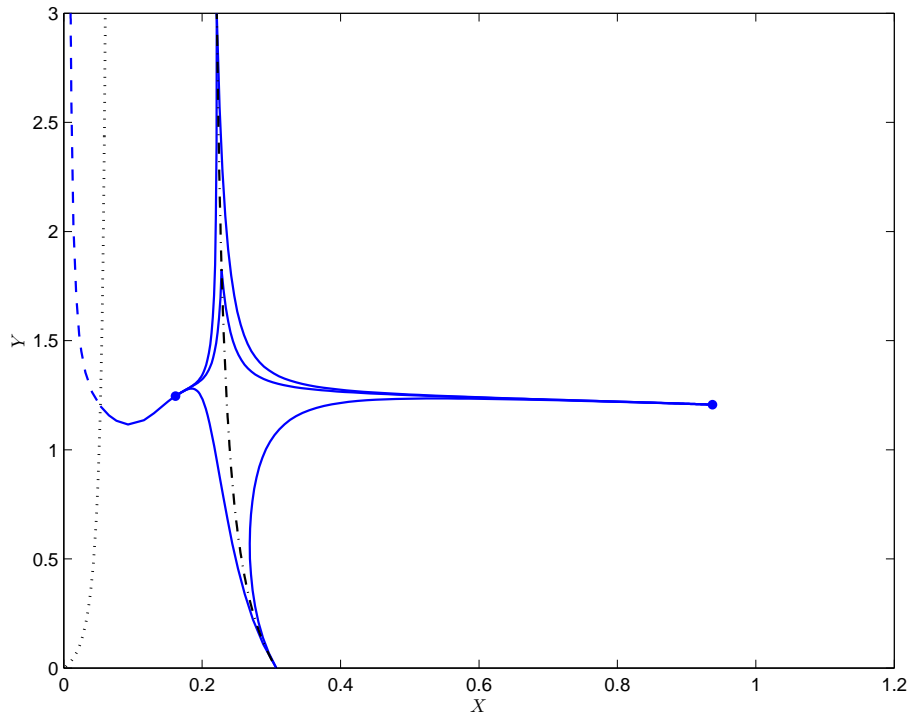


**Figure 5.29:** Indifference curve. The phase portrait of the indifference case includes both equilibria (*dots*), some characteristic trajectories (*dark curves*), the boundary curve (*dotted*), the continuation of a path in a non-admissible area (*dashed*), and the indifference curve (*dot-dashed*).

as only the poor citizens contribute to the objective function, i.e., the government does not benefit directly from middle-class families. In the left case, the level of  $X$  is very low. Therefore, the social advancement described by  $\left(\frac{kX(t)}{kX(t)+Y(t)}\right)^e$  is as well on a sufficiently low level for  $Y$  not to shrink too much due to social integration (Note, that the whole social advancement term is given by  $\gamma Y(t) \left(\frac{kX(t)}{kX(t)+Y(t)}\right)^e$ ), which would be counter-productive in the given parametrization ( $\rho_X = 0$ ).

**Table 5.4:** Equilibria in the case of indifference.

	left steady state	right steady state
$X$	0.1616	0.9374
$Y$	1.2461	1.2066
$\lambda_1$	0.2636	-0.031
$\lambda_2$	0.5016	0.5092

Figure 5.30 enables an interesting observation considering the optimal levels of the

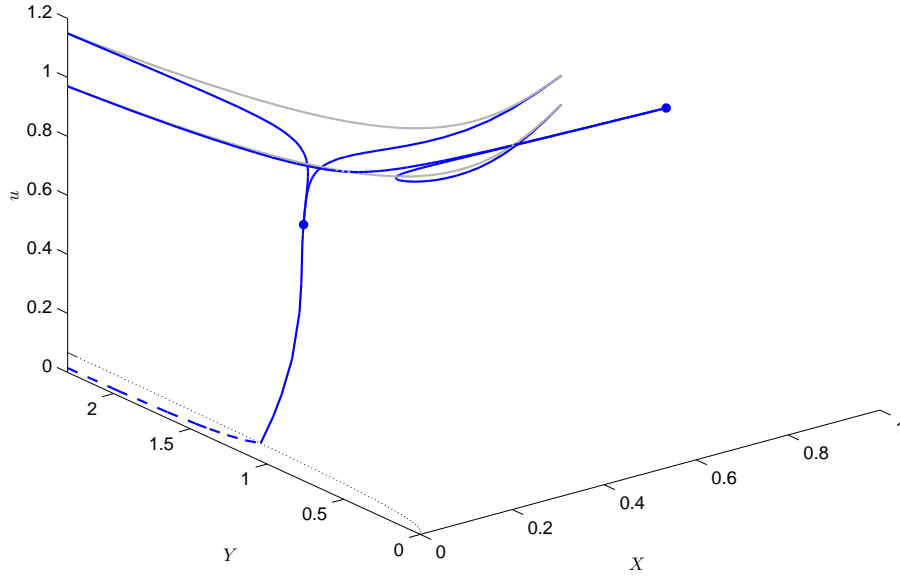


**Figure 5.30:** Indifference curve 3D.

**Fig. 5.30** The phase portrait is a 3D illustration of Fig. 5.29 containing both equilibria (*dots*), some characteristic trajectories (*dark curves*), the boundary curve (*dotted*), the continuation of a path in a non-admissible area (*dashed*) and two branches of the indifference curve (*gray*) correspond to the two different initial control values, when starting on the indifference curve and converging to either of two equilibria. Converging to the left equilibrium requires more control than converging to the right equilibrium.

control on the indifference curve. The two gray branches of the indifference curve correspond to the two different initial control values, when starting on the indifference curve and converging to either of the two equilibria. It is obvious that converging to the left equilibrium requires more control than converging to the right equilibrium. The left equilibrium has a very low level of middle-class families but the level of poor families is higher than in the right equilibrium. In the right equilibrium, the level of middle-class people exceeds the level in the left steady state about six times, but it is still under its own car-

rying capacity. In other words, the optimal trade-off for the government when converging to the left equilibrium is to apply an intensive control, that is to invest, and then to profit from the higher level of poor families. On the other hand, in the right equilibrium the decision maker profits from the higher level of middle-class people by using a lower control.

Summing up this case, the indifference curve separates two steady states in which the neighborhood is dominated by poor families. One of these states reflects a “ghettoing” scenario as showing an underpopulation of middle-class. For further information read on (Grass and Tragler, 2010, Chap. 4.1).

The following passage describes how to actually calculate indifference curves with OCMat. After calculating the two equilibria, the user should calculate the corresponding stable paths<sup>18</sup> by using

```
initStruct=initoccont('extremal',m, 'initpoint',1:2,ocEP{1}.dynVar(1:2,1),
ocEP{2},'IntegrationTime',500);
opt=setocoptions('OCCONT','InitStepWidth',0.01/5^4 , 'MaxStepWidth' ,0.01,
'MeanIteration',50,'OC','BVPSolver','bvp5c');19
[sol soln]=occont(m,initStruct,opt);
m=store(m)20

initStruct=initoccont('extremal',m,'initpoint',1:2,ocEP{2}.dynVar(1:2,1),
ocEP{1},'IntegrationTime',500);
[sol soln]=occont(m,initStruct,opt);
m=store(m)
```

and the corresponding Hamiltonians of the stable paths, followed by the intersection of the Hamiltonians by using

```
dnss=finddnss(m,1,2)
dnss = 0.2282
      1.2427
```

whereby 1,2 symbolizes the first and the second so-called slice manifolds. For the intersection of the Hamiltonians it is assumed that there is an overlapping region on the stable paths for which both solutions exist (see Figure 5.31). The Hamiltonian evaluated

---

<sup>18</sup>Note, if one of the continuation processes between the equilibria is successful, the corresponding path is superior and no asymptotic indifference point exists.

<sup>19</sup>Notice the recommended options.

<sup>20</sup>Never forget to store after the continuation process.

along the slice manifold returns the objective function value of the corresponding solution (up to the factor  $\frac{1}{r}$ ).

The set of commands

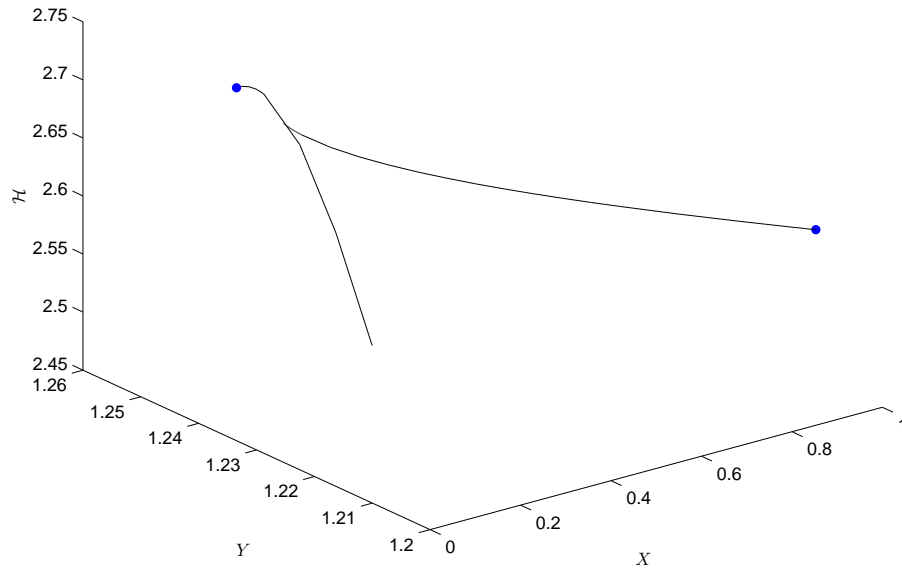


**Figure 5.31:** Intersection of the Hamiltonians.

```
clf,type='hamiltonian';coordinate=1;statecoordinate1=1;statecoordinate2=2;
plot3phaseocresult(m,type,statecoordinate1,statecoordinate2,coordinate,
'only',{'SliceManifold'},'onlyindex',{[]},'continuous','off','limitset','off',
'Color',[0.4 0.4 0.4]),hold on;
plot3phaseocresult(m,type,statecoordinate1,statecoordinate2,coordinate,
'only',{'Equilibrium'},'onlyindex',{[]},'limitset','on','Marker','.',
'MarkerSize',16), hold off,figure(gcf)
```

enables a 3D plot of the slice manifold together with the equilibria.

Thereafter, the user can calculate the stable paths starting at the intersection point by using:

```
ocEx=extremalsol(m);
initStruct=initoccont('extremal',m, 'initpoint',1:2,dnss,ocEx{1});
[sol soln]=occont(m,initStruct,opt);
m=store(m);
```

```

initStruct=initoccont('extremal',m, 'initpoint',1:2,dnss,ocEx{2});
[sol soln]=occont(m,initStruct,opt);
ocEx=extremalsol(m);

```

and generate the “dnss object” by calling

```
ocD=[ocEx{3} ocEx{4}];
```

For the purpose of calculating the indifference curve, the user has to initialize the BVP knowing an approximate initial value from the previous Hamiltonian intersection procedure.

```

initStruct=initoccont('dnss',m, 'initpoint',2,0, ocD); 21
[sol soln]=occont(m,initStruct,opt); soln m=store(m)

initStruct=initoccont('dnss',m, 'initpoint',2,3, ocD);
[sol soln]=occont(m,initStruct,opt); soln m=store(m)

```

The signal word for the calculation of the indifference curve is `dnss`. In the underlying case, 2 determines the coordinate to be fixed (COOR), while 0 and 3 provide the values of the fixed coordinate (VAL). `ocD` is the initial function given by a vector generated above. To plot other characterizing trajectories the user has to re-call the previous initialization and vary the value of the fixed coordinate. For more information read on (Grass, 2010-2011, Lecture 4).

After this general analysis of a spacial case of indifference the next interesting question is, if there exist more moderate sets of parameters, which also reveal an indifference case. In the next section such a case will be presented.

## 5.5 From base case to case of indifference

To illustrate a case of indifference we used a somewhat unrealistic parametrization, which deviates significantly from the base case (see Table 5.3). In particular, the discount rate  $r$  differs from its base case value by the factor of 20,  $\sigma$  is multiplied by the factor of 100, the objective function coefficient on  $X$ ,  $\rho_X$ , is even set to zero, and the objective function coefficient on  $Y$ ,  $\rho_Y$ , is extremely high. Moreover, the cost coefficient is halved in the case of indifference compared to the base case, and the assimilation coefficient  $\gamma$  is increased by more than 10%. The purpose of this section is to find a more moderate parametrization,

---

<sup>21</sup>The general command is `initStruct=initoccont('dnss',m,'initpoint',COOR,VAL,INITSOL);`

for which such a complex and mathematically interesting behavior occurs.

A series of analyses on the system parameters summarized in Table 5.5 reveals parameter settings which exhibit indifference points, but are way closer to base case parameters. Based on the indifference case from Section 5.4 but doubling the cost coefficient  $c$  and reducing the assimilation coefficient  $\gamma$  to 0.45, i.e., resetting them to base case values, the new calculation shows another indifference case. As expected, by rising costs and lowering assimilation in the right equilibrium we find a higher optimal level of middle class families, while the level of poor people becomes lower. However, in the left equilibrium the level of middle class people as well as the level of poor families are lower than in the indifference case discussed in Section 5.4.

Next, the weight on the objective function control terms,  $\sigma$ , will be changed additionally, i.e., a reset to  $\sigma = 0.01$ , which means a division by one hundred. As expected, it influences the behavior of the system crucially and results in a single solution with a very low optimal level of middle-class people and an extremely high level of poor people.

Obviously, it is of particular interest to find out, what happens to the equilibria on the way from  $\sigma = 1$  (case of indifference) to  $\sigma = 0.01$  (unique optimal solution). For  $\sigma = 1$ , the canonical system has three equilibria (see Table 5.5 and Figure 5.32). Two of them have a two-dimensional stable manifold<sup>22</sup>, i.e.,  $(X, Y) = (0.0806, 1.1443)$  and  $(X, Y) = (1.0175, 1.0762)$ , while the third equilibrium i.e.,  $(X, Y) = (0.3282, 1.3663)$  has only a one-dimensional stable manifold, which is therefore of no further interest regarding the optimal system. For  $\sigma = 0.01$ , there is only one equilibrium, which is  $(X, Y) = (0.2855, 1.3432)$ . We hence expect that somewhere on the way from  $\sigma = 1$  to  $\sigma = 0.01$  an equilibrium with one-dimensional stable manifold collides with an equilibrium with two-dimensional stable manifold to annihilate each other, i.e., a saddle-node-bifurcation<sup>23</sup> occurs. This is indeed the case, as illustrated in Figure 5.32.

**Table 5.5**

$\sigma$	$X$	$Y$	No. of $Re\xi < 0$
1	0.0806	1.1443	2
1	0.3282	1.3663	1
1	1.0175	1.0762	2
0.01	0.2855	1.3432	2

Except for the base case scenario all the other cases described above address the eco-

---

<sup>22</sup>These two equilibria cause an indifference case, i.e., both of them are locally optimal and there are points for which the decision-maker is indifferent, which one to choose.

<sup>23</sup>Another name for saddle-node-bifurcations is blue sky bifurcation.



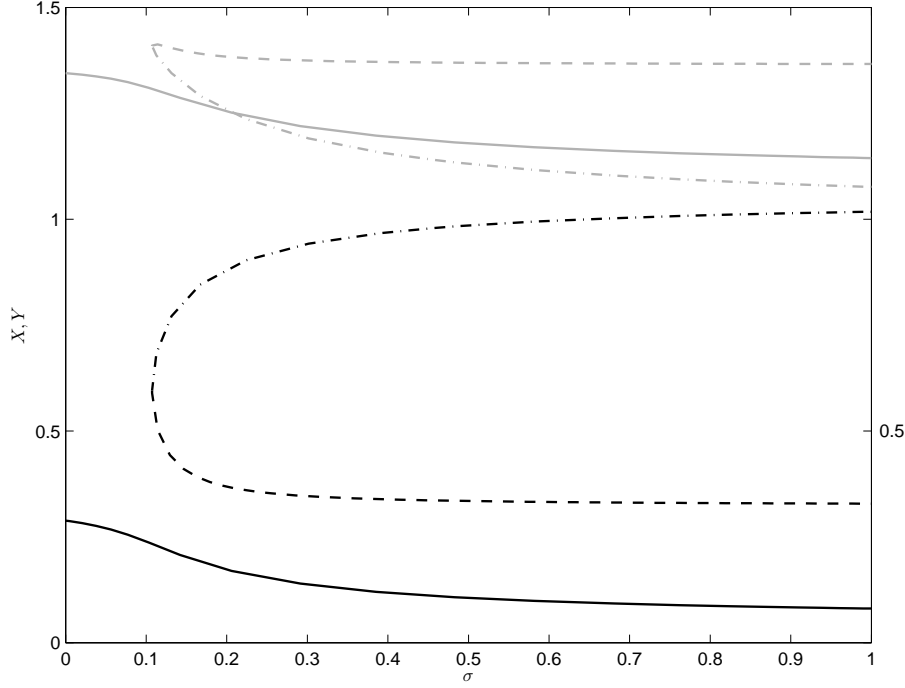


**Figure 5.32:** Saddle-Node-Bifurcation.  $X(\sigma)$  (*black*),  $Y(\sigma)$  (*gray*). Considering  $\sigma = 1$  the path starting at  $(X, Y) = (0.0806, 1.1443)$  is a *line*, the path starting at  $(X, Y) = (0.3282, 1.3663)$  is *dashed*, and the path starting at  $(X, Y) = (1.0175, 1.0762)$  is *dotdashed*. By varying  $\sigma$  from 1 to 0.01 the dynamics of the canonical system change from three equilibria to only one equilibrium. A local bifurcation occurs in which an equilibrium with one-dimensional stable manifold collides with an equilibrium with two-dimensional stable manifold.

nomically and politically unrealistic situation, in which the decision-maker does not value the presence of middle-class families, i.e., the relative benefit per unit of time of  $X$  is equal to zero,  $\rho_X = 0$ . For the purpose of realistic applicability of the underlying model it is necessary to consider a positive objective function coefficient on  $X$ . For instance,  $\rho_X = 0.001$  and  $\rho_Y = 0.02$  describes a scenario, in which the presence of middle-class people is regarded, albeit to a very modest extent. More precisely the social benefit derived from the presence of poor people is twice as high as in the base case and 20 times as high as the benefit from middle-class families. The analysis reveals again an indifference case. A sensitivity analysis on  $\rho_X$  shows that even the smallest increase on  $\rho_X$  eliminates indifference. However, it is possible to reduce the objective function coefficient on  $Y$  to  $\rho_Y = 0.012$  without changing the dynamic behavior of the system.

It is further interesting to observe the dynamic behavior of the system by equalizing  $\rho_X$  and  $\rho_Y$ , where a unique solution occurs. Comparing the results of the scenario with  $\sigma = 0.01$ ,  $\rho_Y = 0.02$ ,  $\rho_X = 0.001$ , and  $r = 1$  with the same scenario only varying the discount rate  $r$ , which means resetting it to its base case value  $r = 0.05$ , two similar indifference cases appear. As already noted above, the effect of varying of the time discount

rate  $r$  is almost negligible.

The last column of the Table 5.6 shows the most moderate parametrization found so far, which reveals an indifference case. The only remaining crucial difference is probably the low value of  $\rho_X$ .

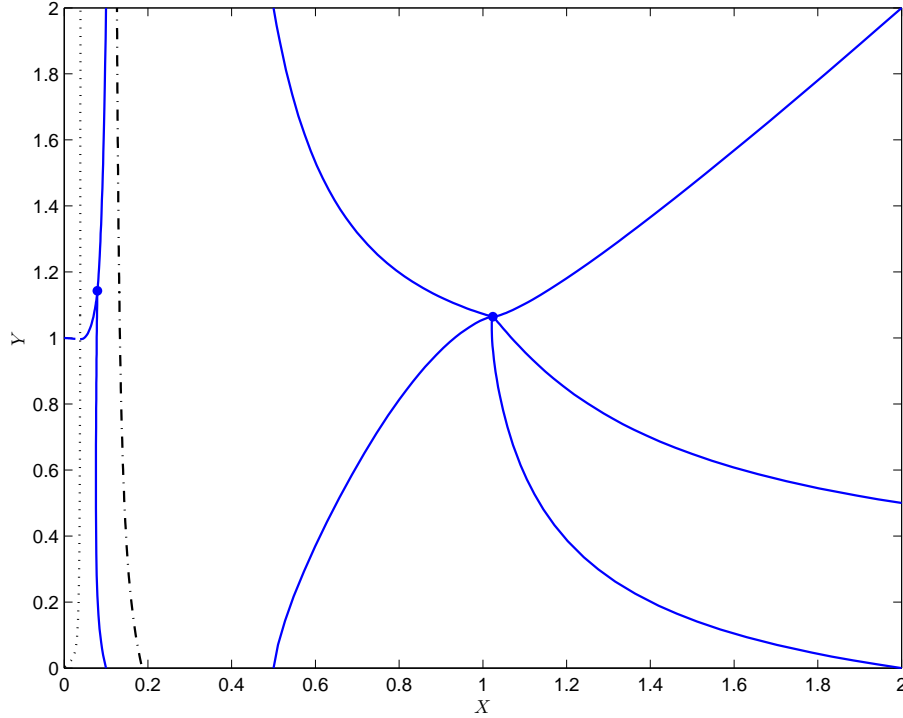


**Figure 5.33:** Indifference Case with moderate parametrization. The phase portrait of the indifference case includes both equilibria (*dots*), some characteristic trajectories (*dark curves*), the boundary curve (*dotted*), the continuation of a path in a non-admissible area (*dashed*), and the indifference curve (*dotdashed*). The area with zero control is comparatively small.

Summing up the cases of indifference, the calculations reveal optimal population mixes dominated by poor families, which may even be underpopulated with respect to middle-class families (see left equilibria), i.e., “ghettoing” scenarios. As in the base case, no control should be applied for low enough numbers of middle-class people, but the region with zero control is significantly smaller, see Figure 5.33.

The main result of this section is the revelation of a parameter set which is most similar to the base case, differing only in the two parameters  $\rho_X$  and  $\rho_Y$  but exhibiting a case of indifference. The main difference is the interchanging of the emphasis on the benefit derived directly from the presence of middle-class people and the indirect benefit caused by poor citizens settled down in the middle-class area.

**Table 5.6:** From base case to case of indifference.

Parameter	Base Case	Different Scenarios						
$r$	0.05	1	1	1	1	1	0.05	0.05
$\rho_X$	0.02	0	0	0	0	0.001	0.001	0.001
$\rho_Y$	0.01	2	2	2	0.02	0.02	0.02	0.012
$\sigma$	0.01	1	1	0.01	0.01	0.01	0.01	0.01
$c$	2	1	2	2	2	2	2	2
$\gamma$	0.45	0.5	0.45	0.45	0.45	0.45	0.45	0.45
$a$	2	2	2	2	2	2	2	2
$b$	2	2	2	2	2	2	2	2
$d$	1	1	1	1	1	1	1	1
$\beta$	0.5	0.5	0.5	0.5	0.5	0.5	0.5	0.5
$k$	1	1	1	1	1	1	1	1
$e$	1	1	1	1	1	1	1	1
Coordinates	Equilibria							
$X^1$	1.0485	0.1616	0.0806	0.2855	0.0806	0.0833	0.0949	0.0795
$Y^1$	1.0141	1.2461	1.1443	1.3432	1.1443	1.1482	1.1645	1.1427
$\lambda_1^1$	0.0091	0.2636	0.2051	0.8551	0.0021	0.0011	0.0009	0.0004
$\lambda_2^1$	0.005	0.5016	0.5589	0.4586	0.0056	0.0056	0.0074	0.0046
$X^2$		0.9374	1.0175		1.0175	1.0184	1.0063	1.0239
$Y^2$		1.2066	1.0762		1.0762	1.0746	1.0961	1.0644
$\lambda_1^2$		-0.031	-0.024		-0.0002	0.0001	0.00002	0.0002
$\lambda_2^2$		0.5092	0.5856		0.0059	0.0059	0.0079	0.00497

The following chapter provides a summary of the results presented in this thesis and discusses practical policy implications.

## Summary and Policy Conclusions

The main purpose of the present work was to determine how a social planner can optimally integrate a stream of poor families into a middle-class area without evoking middle-class flight. We found probably all possible scenarios, in which either a low level of control, no control at all, or a high governmental intervention is optimal. The highest level of social intervention is occurs for a large objective function coefficient on  $Y$ ,  $\rho_Y$ , i.e. by a relatively high direct valuation of the presence of marginal families. Likewise, it is not surprising that for low control costs,  $c$ , the optimal trade-off is to invest a lot. Very interesting is the result, where even for extremely high costs a certain level of control is optimal.

On the other hand, if the flight coefficient rate  $\beta$  is very high, the strategy of no intervention is optimal, i.e., not to place poor families into the concerned area. Also for a small growth rate of the middle-class population it is advisable to reduce the control considerably.

The parameter  $\rho_X$ , which describes how the decision-maker values the presence of established middle-class families, influences the system dynamics considerably. If the social planner assumes a big economic value from middle-class people, the integration of poor families goes down.

The positive effect of the influx of marginalized people in a settled community stems from the advancement due to social assimilation, as described by the term

$$\gamma Y(t) \left( \frac{kX(t)}{kX(t) + Y(t)} \right)^e.$$

The assimilation coefficient  $\gamma$  reflects part of the rate at which families initially placed in a middle-class neighborhood established middle-class status, i.e., the “success” rate for people who participate in housing mobility programs. That such an assimilation can occur is an underlying premise of our model.

If the level of assimilation is very low, the optimal policy is not to invest too much. In such a case, the optimal level of middle-class families is under its saturation level ( $= 1$ ),  $Y$  is above it. Considering a very high assimilation coefficient,  $X$  exceeds 1 while  $Y$  falls below its saturation level, thus a substantial control is advisable. Varying the assimilation coefficient  $\gamma$ , no tipping behavior occurs.

Surprisingly, the effect of a change in the social integration coefficient  $k$  on the optimal control is very low, i.e., the level of optimal control is almost constant for a wide range of  $k$ .

Considering a quadratic social advancement term (i.e.,  $e = 2$  unlike the base case  $e = 1$ ), the optimal level of poor families exceeds the optimal level of middle-class people, and the optimal control is about 25% lower than in the base case.

Naturally, the time discount rate  $r$  is a very crucial quantity regarding the system dynamics, describing the measure of focusing on the future versus focusing on the presence. Against all expectations, changing  $r$  has hardly any effect on the unique equilibrium of the canonical system when considering the base case parameter set presuming  $\rho_X > \rho_Y$ . Similarly modest is the impact of  $\sigma$ , the weight on objective function control terms, on the solution of the canonical system.

The own “natural” dynamics of the populations middle-class residents and poor families are described by the logistic growth rates  $a$  and  $b$ , respectively. Their impact on the optimal solution is according to expectations. The higher the growth rate of the middle-class population, the higher the optimal control. On the opposite, the higher the growth rate of poor people, the less it is optimal to integrate poor families into the middle-class neighborhood.

The valuation of the presence of middle-class people versus on the presence of poor people is one of the main driving factors of the model. The fundamental analysis took place under the assumption  $\rho_X > \rho_Y$ . In the base case,  $\rho_X$  is twice as big as  $\rho_Y$ . Omitting this assumption reveals interesting results. If the decision maker is primarily concerned about marginalized families, the occurrence of multiplicity for some initial states is possible. For these initial states, which constitute the indifference curve, there are multiple optimal solutions, thus the decision-maker is indifferent about which to choose. One analyzed indifference case discussed above, for which  $\rho_X = 0.001$  and  $\rho_Y = 0.012$ , reveals two locally optimal population mixes, both of which are dominated by poor families. One of the optimal equilibria even exhibits an underpopulation of middle-class. The almost vertical indifference curve describes initial points for which the level of middle-class people is about 80% under its saturation level. In other words, in such a “ghettoing” scenario

turns out to be optimal, which we would expect to be non-diserale in the real world.

# List of Figures

3.1	Placing the poor to the middle-class neighborhood . . . . .	17
5.1	Phase portrait . . . . .	32
5.2	2D phase portrait with boundary curve . . . . .	34
5.3	3D phase portrait with boundary curve . . . . .	35
5.4	Discount rate $r$ . . . . .	36
5.5	Maximal growth rate $a$ at $X = 0$ . . . . .	38
5.6	Maximal growth rate $b$ at $Y = 0$ . . . . .	38
5.7	Program cost coefficient $c$ . . . . .	39
5.8	Program cost coefficient $c$ on different intervals . . . . .	41
5.9	Flight coefficient beta . . . . .	42
5.10	Non-monotonic dependence of $X$ on beta . . . . .	43
5.11	Left maximum . . . . .	44
5.12	Left intersection . . . . .	44
5.13	Base case . . . . .	45
5.14	Minimum of $X$ . . . . .	45
5.15	Right intersection . . . . .	46
5.16	Right maximum . . . . .	46
5.17	Assimilation coefficient . . . . .	47
5.18	Exponent in the social advancement term . . . . .	48
5.19	Objective function coefficient $\rho_X$ . . . . .	48
5.20	Objective function coefficient on $X$ in the state-control space . . . . .	49
5.21	Objective function coefficient $\rho_X$ , zoom . . . . .	49
5.22	Objective function coefficient $\rho_Y$ . . . . .	50
5.23	Objective function coefficient $\rho_Y$ in the state-control space . . . . .	51
5.24	Objective function coefficient on $Y$ , zoom . . . . .	51
5.25	Carrying capacity of $Y$ . . . . .	52
5.26	Social integration coefficient . . . . .	53
5.27	Weight on objective function control terms . . . . .	53
5.28	Weight on objective function control terms in the state-control space . . . . .	54
5.29	Indifference curve . . . . .	57
5.30	Indifference curve 3D. . . . .	58



5.31	Hamiltonian . . . . .	60
5.32	Saddle-Node-Bifurcation . . . . .	63
5.33	Indifference Case with moderate parametrization . . . . .	64

# List of Tables

3.1	Base case model parameters. . . . .	19
5.1	Slopes of equilibria values of $X$ , $Y$ , and $u$ as functions of the parameters. . . .	55
5.2	Parameter set exhibiting indifference points. . . . .	56
5.3	Comparison of parameter values on base case vs. indifference case. . . . .	56
5.4	Equilibria in the case of indifference. . . . .	58
5.5	Saddle-Node-Bifurcation . . . . .	62
5.6	From base case to case of indifference . . . . .	65

# Bibliography

- R. Bernstein and T. Edwards. An older and more diverse nation by midcentury. *U.S. Census Bureau*, August, 14 2008. URL <http://www.census.gov/newsroom/releases/archives/population/cb08-123.html>.
- J.R. Betts and R.W. Fairlie. Does Immigration Induce ‘Native Flight’ from Public Schools into Private Schools? *Elsevier, Journal of Public Economics Journal*, 83:987–1012, 2003.
- United States Census Bureau. Annual estimates of the population of metropolitan and micropolitan statistical areas: April 1, 2000 to july 1, 2008 (cbsa-est2008-01). In *Population Division*, March 19, 2009. URL <http://www.census.gov/popest/metro/CBSA-est2008-annual.html>. September 18, 2011, Vienna.
- United States Census Bureau. Resident population by sex, race, and hispanic origin status: 2000 to 2009. In *Statistical Abstract of the United States*, 2011a. URL <http://www.census.gov/compendia/statab/2011/tables/11s0006.pdf>.
- United States Census Bureau. U.S. Popclock Projection. In *U.S. & World Population Clocks*, 2011b. URL <http://www.census.gov/population/www/popclockus.html>. September 17, 2011 20:00, Vienna.
- J.P. Caulkins, G. Feichtinger, G. Tragler, D. Behrens, and S. Bushway. Population dynamics model. Memo #26, 1999.
- J.P. Caulkins, G. Feichtinger, D. Grass, M. Johnson, G. Tragler, and Y. Yegorov. Placing the poor while keeping the rich in their place: Separating strategies for optimally managing residential mobility and assimilation. *Demographic Research*, 13(1):1–34, 2005a.
- J.P. Caulkins, G. Feichtinger, D. Grass, and G. Tragler. A model of moderation: Finding Skiba points on a slippery slope. *Central European Journal of Operations Research*, 45-64(1):13, 2005b.
- C. T. Clotfelter. Are whites still fleeing? racial patterns and enrollments shifts in urban public school. *Journal of Policy Analysis and Management*, 20(2):199–221, 2001.

- C. T. Clotfelter. *After Brown: The Rise and Retreat of School Desegregation*. Princeton University Press., 2004.
- D.W. Deckert and K. Nishimura. A complete characterization of optimal growth paths in an aggregated model with nonconcave production function. *Journal of Economic Theory*, 31:332–354, 1983.
- C. DeNavas-Walt, B.D. Proctor, and J.C. Smith. Income, poverty, and health insurance coverage in the united states: 2008. *U.S. Census Bureau*, 2008.
- H. Elhassan, J. Feins, J. Goering, H.J. Holin, J. Kraft, and D. McInnis. Moving to opportunity for fair housing demonstration program: Current status and initial findings. Technical report, U.S. Department of Housing and Urban Development Office of Policy Development and Research, 1999. URL <http://www.huduser.org/publications/pdf/mto.pdf>.
- I.G. Ellen. Sharing america’s neighborhoods: The prospects for stable, racial integration. Technical report, Harvard University Press, 2000.
- R.W. Fairlie. Private schools and ‘latino flight’ from black schoolchildren. *Demography*, 39(4):655–674, 2002.
- G. Feichtinger and R.F. Hartl. *Optimale Kontrolle ökonomischer Prozesse: Anwendungen des Maximumprinzips in den Wirtschaftswissenschaften*. Walter de Gruyter, Berlin, 1986. URL <http://www.univie.ac.at/bwl/prod/hp/hartl/FeiHaBook/OCOP.pdf>.
- M. Fujita. *Urban Economic Theory: Land Use and City Size*. Cambridge University Press, 1989.
- F. Gaschet and N. Gaussier. Urban segregation and labour markets within the bordeaux metropolitan area: an investigation of the spatial friction. Technical report, Université Montesquieu-Bordeaux IV, 2004.
- D. Grass. *OCMat: A MATLAB package for the analysis of optimal control problems*. Operations Research and Control Systems (ORCOS), Vienna University of Technology, 2010-2011. URL <http://orcos.tuwien.ac.at/research/ocmat-software>.
- D. Grass and A. Seidl. *OCMat Manual*, 2008.
- D. Grass and G. Tragler. Optimal dynamic management of the population mix. *Central European Journal of Operations Research*, 18(4):539–551, 2010.
- G. Grass, J.P. Caulkins, G. Feichtinger, G. Tragler, and D.A. Behrens. *Optimal Control of Nonlinear Processes: With Applications in Drugs, Corruption, and Terror*. Springer Verlag, Berlin, 2008.

- V. Henderson. The sizes and types of cities. *American Economic Review*, 64:640–656, 1974.
- F. Kemper. Restructuring of housing and ethnic segregation: Recent developments in berlin. *Urban Studies*, 35(10):1765–1789, October 1998.
- S.E. Mayer and C. Jencks. Poverty and the distribution of material hardship. *Journal of Human Resources*, 24(1):88–114, 1989.
- G. Meen, K. Gibb, J. Goody, T. McGrath, and J. Mackinnon. *Economic segregation in England: causes, consequences and policy*, volume ISSN 0958-3084. Joseph Rowntree Foundation, December 2005.
- Bureau of Labor Statistics. Employment situation summary. In *Economic News Release*, August, 2011. URL <http://www.bls.gov/news.release/empsit.nr0.htm>. September 18, 2011.
- Bureau of Labor Statistics. Labor force statistics from the current population survey. In *Unemployment Rate*, August, 2011. URL <http://www.bls.gov/cps/>. September 18, 2011, Vienna.
- Die Presse. Österreich ist EU-Land mit niedrigster Arbeitslosigkeit. August 31, 2011. URL [DiePresse.com](http://www.diepresse.com). > Wirtschaft > National.
- T. Schelling. Dynamic models of segregation. *Journal of Mathematical Sociology*, Vol. 1, 1971. Abbreviated version appeared as “Models of Segregation”, in *The American Economic Review*, Vol. LIX, No. 2, May 1969.
- B. Schindler Rangvid. Living and learning separately? ethnic segregation of school children in copenhagen. *Urban Studies*, 44(7):1329–1354, June 2007.
- S.P. Sethi. Nearest feasible paths in optimal control problems: Theory, examples, and counterexamples. *Journal of Optimization Theory and Applications*, 23:563–579, 1977. 4, Dec. 1977.
- S.P. Sethi. Optimal advertising policy with the contagion model. *Journal of Optimization Theory and Applications*, 29:615–627, 1979. 4, Dec. 1979.
- A.K. Skiba. Optimal growth with a convex-concave production function. *Econometrica*, 46:527–539, 1978.
- P. Starr. A new deal of their own. *American Prospect*, February 25, 2008.
- UNICEF. Child poverty in perspective: An overview of child well-being in rich countries. *Innocenti Research*, Report Card 7, 2007. URL [http://www.unicef-irc.org/publications/pdf/rc7\\_eng.pdf](http://www.unicef-irc.org/publications/pdf/rc7_eng.pdf).

G. Verdugo. Public housing and residential segregation of immigrants in france, 1968-1999. *IZA Discussion Paper*, IZA Discussion Paper No. 5456, 2011.